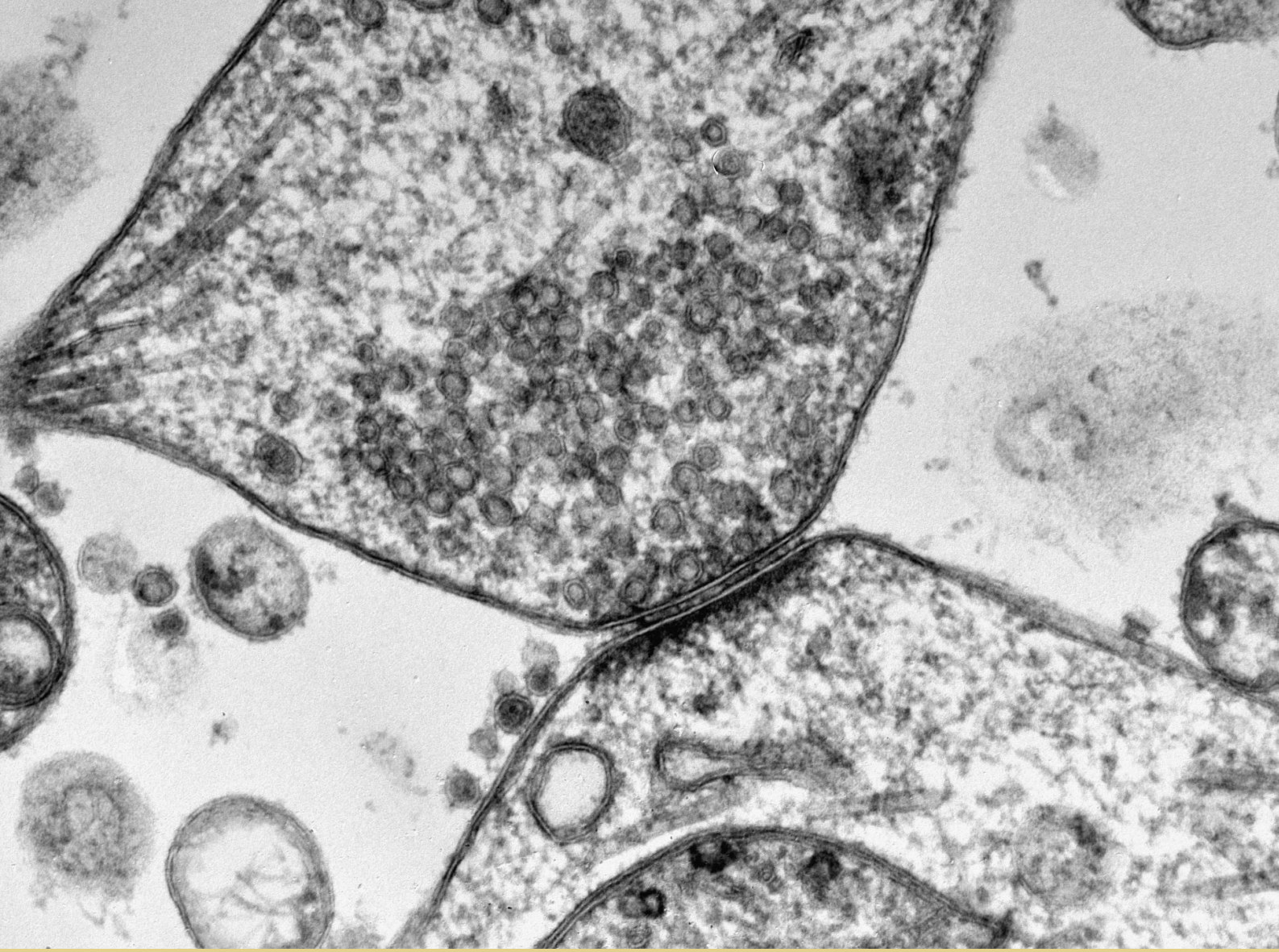

Débora Carolina Garrido Cruz

Analysis of Shank2/Shank3 loss during neuronal development

Dissertação de Mestrado em Biologia Celular e Molecular, Área de Especialização em Neurobiologia, orientada pelo Professor Doutor Tobias M. Böckers e pela Doutora Ana Luísa Monteiro de Carvalho e apresentada ao Departamento de Ciências da Vida da Faculdade de Ciências e Tecnologia da Universidade de Coimbra.

Julho 2017

· U C ·

Universidade de Coimbra

Analysis of Shank2/Shank3 loss during neuronal development

Débora Carolina Garrido Cruz

UNIVERSIDADE DE COIMBRA

Master in Cellular and Molecular Biology
Specialization in Neurobiology

MSc Dissertation

Dissertation submitted to the Department of Life Sciences of the University of Coimbra to meet the necessary requirements for the degree of Master of Cellular and Molecular Biology with specialization in Neurobiology, under supervision of Professor Doctor Tobias M. Böckers (Universität Ulm, Germany) and Doctor Ana Luísa Monteiro de Carvalho (Universidade de Coimbra, Portugal).

2016-2017

This project was supported by the Institut für Anatomie und Zellbiologie at Universität Ulm and IMI-EU-AIMS FP7/Programme N115300

Acknowledgments

Prof. Dr. Tobias Böckers, thank you for giving me the chance to work in your institute and to develop this exciting project. I am grateful for all the advice, work discussions and especially for sharing your passion and enthusiasm for science with me. This experience definitely enriched my academic background.

Dr. Ana Luísa Carvalho, thank you for supporting me and for all the advice, especially during the *Seminários*.

Dr. João Peça, thank you for recommending me to do my Master Thesis at the Institut für Anatomie und Zellbiologie. It was absolutely the right choice.

Alberto Catanese, it is a great pleasure to be "your student". Thank you for sharing your knowledge with me, for helping me every single day, for all the work discussions, for trusting me, for your unlimited patience, (…) and for supporting me. I could not ask for anything better. Thank you very much!

PD Dr. Jürgen Bockmann, Maria Manz and Ursula Pika-Hartlaub, thank you for supporting me with *Shank2*$^{flx/flx}$ *Shank3*$^{flx/flx}$ mice experiments.

To everyone in the institute, thank you for welcoming me, for being always available to help me and for all the good moments.

Prof. Dr. Paul Walther and collaborators, thank you for your help with the preparation of biological specimens for Transmission Electron Microscopy.

Sertap, Judy and Marvin, thank you so much for helping me to feel integrated so quickly. Thank you for all the good moments outside the lab and for teaching me German.

Rita, quem te tem como amiga, tem quase tudo. Mesmo à distância, obrigada pelos "momentos Monlou", pelos teus sábios conselhos e por continuares a ser uma preciosa ajuda a resolver todos meus problemas informáticos.

Margarida, João, Belinha, (Dr.) Miguel Cardoso, Carina, Soraia, Laura, Graça e Cris obrigada pela vossa amizade, carinho, motivação e por fazerem parecer que a Alemanha não fica assim tão longe de Portugal como parece.

Pais, o vosso apoio, carinho e motivação foi crucial para ser bem-sucedida durante esta desafiante experiência. Em poucas palavras, nada teria sido possível sem vocês. Muito obrigada!

Agora como minha melhor amiga, obrigada Sandra pela liberdade e pelo apoio incondicional que me deste e continuas a dar em todas as opções pessoais e profissionais que me permitem ser quem sou.

E, claro, também te agradeço a ti grande amiga, que sem nunca perceber o motivo da minha ausência me enches de felicidade sempre que regresso a casa.

Table of Contents

Abstract

Autism Spectrum Disorders (ASDs) are heterogeneous neuropsychiatric pathologies characterized by different core features such as repetitive behaviours, language impairment and difficulties in social interactions. In the last years several lines of evidences have pointed out the key contribution of synaptic impairments in this particular diseases. Moreover, several genes, which happen to be mutated in ASDs, encode for synaptic proteins such as Shanks. Although alterations at the synaptic microenvironment appear to strongly contribute in ASDs pathogenesis, the biological and molecular mechanisms affecting these specific neuronal structures are still poorly understood.

To better understand how synaptic impairment might influence those behavioural traits that are impaired in ASDs, we investigated the role of two major scaffold proteins at the synapse: Shank2 and Shank3. Those two proteins are mutated in some monogenicforms of ASD, giving us the possibility to investigate synaptic alterations that might specifically contribute to the pathogenesis of neuropsychiatric disorders.

To this end, we investigated the contribution of Shanks in synaptic morphological changes through Transmission Electron Microscopy under *non-conventional* synaptic plasticity induction (starvation). In addition, we performed canonical immunohistochemistry analysis to better elucidate the changes occurring with respect to different synaptic markers that could be triggered by alterations in Shank family members. Moreover, to point out the specific role of Shank2 and Shank3 in the maintenance of a physiological synaptic environment and in a proper synaptic development, we established primary neuronal cultures from a novel conditional Shank2-3 double KO mouse model. This *in vitro* system was used to knock down the expression of the two scaffold proteins at different stages of cultivation to investigate the specific contribution of Shanks during neurodevelopment and synaptogenesis.

Interestingly, while Shank3 seems to be unaffected to synaptic remodelling by starvation we observed a slight down-regulation of Shank2. Although both scaffolding proteins share similar domain composition, these data highlight the idea that distinct elements of the same Shank protein family might contribute to different synaptic signalling pathways. Nevertheless, the well-described Shank binding-partner Homer was found stabilized at synapses even when the ultrastructural postsynaptic density (PSD) architecture was seen to dramatically reduce in response to synaptic remodeling induction. In contrast, the absence of both Shank2 and Shank3 proteins seems to compromise the assembly of Homer into new synaptic contacts. Taken together, these findings indicate that in addition to providing synaptic dynamics, Shank scaffolding proteins also play a crucial role in stabilizing the molecular synaptic composition.

We also provided evidences that the postsynaptic abnormalities induced by Shank2 and Shank3 loss at early stages of development lead to an up-regulation of the presynaptic scaffolding protein Bassoon while the opposite effect was observed when Shanks are disrupted at later stages (later on). This, suggests that the disruption of Shank proteins at distinct stages of neuronal development might affect different processes during synaptogenesis.

Furthermore, a variability of phenotypes was also found between distinct cell types. For instance, whereas Shank2 and Shank3 deficient hippocampal neuronal cell cultures seem to undergo dendritic morphological changes, no effects were observed in primary cortical dendritic

arborization complexity, suggesting that distinct cell types could be more vulnerable to Shank loss.
In summary, the investigations provide evidence for neurodevelopment and synaptic alterations in a cell culture system that are depending (i) upon the neuronal cell type, (ii) upon the deletion of a specific Shank family member and (iii) upon the stage of neuronal maturation. The data are important with respect to ASD related developmental alterations of synaptic contacts in Shank model systems that were found to be brain region specific.

Keywords: ASD, Neuronal development, Shank, Synapse, Synaptic plasticity

Resumo

As desordens do Espectro Autista (Autism Spectrum Disorders - ASDs) são patologias neuropsiquiátricas caracterizadas por diferentes sintomas tais como comportamentos repetitivos, défices linguísticos e dificuldade em socializar. Nos últimos anos, diferentes estudos têm revelado que disfunções ao nível das sinapses poderão ser a principal causa para estes sintomas. Além disso, mutações em genes que codificam proteínas sinápticas têm sido reportadas em diferentes casos clínicos de ASD. Embora estas alterações a nível sináptico pareçam ser as que mais contribuem para esta patogénese, os mecanismos biológicos e moleculares pelos quais estas sinapses são afetadas são ainda pouco compreendidos.

Assim, para melhor compreender como é que os défices sinápticos influenciam o desenvolvimento neuronal, o foco do nosso trabalho foi estudar o papel de duas proteínas cruciais na estrutura sináptica: Shank2 e Shank3. Estas duas proteínas encontram-se mutadas em alguns dos casos clínicos de ASD reportados, o que consequentemente nos permite estudar qual a contribuição destas alterações sinápticas para a patogénese de ASDs.

Assim, recorremos à Microscopia Eletrónica para investigar a contribuição das proteínas Shank durante alterações morfológicas ao nível da sinapse, induzidas por um método não convencional (privação de nutrientes). Além disso, realizámos também ensaios imuno-histoquímicos para perceber como é que diferentes marcadores sinápticos são afetados durante o tratamento. Uma vez que estamos também interessados em conhecer o papel destas proteínas a nível fisiológico, estabelecemos culturas neuronais primárias de diferentes regiões cerebrais (hipocampus e córtex) derivadas de um novo modelo animal: murganhos com KO duplo e condicional de Shank2-3. Este sistema *in vitro* foi utilizado para deletar os genes da SHANK2 e da SHANK3 em diferentes estágios de neuro desenvolvimento celular, de forma a mimetizar a falha destas proteínas em diferentes fases do desenvolvimento neuronal e assim investigar a contribuição destas proteínas neste processo.

Curiosamente, observámos que a proteína Shank3 parece não ser afetada pelas alterações sinápticas induzidas pela privação de nutrientes, no entanto, relativamente à proteína Shank2, esta condição parece influenciar negativamente a sua regulação nas sinapses. Embora estas proteínas partilhem estruturas moleculares semelhantes, este resultado é indicador de que existem diferentes elementos da família de proteínas Shank a contribuir para a regulação destas proteínas nas sinapses através de mecanismos celulares distintos. Contudo, a proteína Homer, descrita na literatura como uma das principais parceira das Shanks, encontra-se estabilizada nestas sinapses, mesmo quando a arquitetura da PSD parece ser drasticamente afetada como consequência da remodelação sináptica. Por outro lado, na ausência das proteínas Shank2 e Shank3 o recrutamento e estabilização da proteína Homer ao nível das sinapses parece ser comprometida. Em conjunto, estas observações indicam que além de permitirem plasticidade à sinapse, estas proteínas parecem desempenhar um papel crucial na organização molecular destas estruturas.

Além disso, observámos também que as disfunções sinápticas induzidas pela perda de Shank2 e Shank3, no início do desenvolvimento neuronal, induzem o aumento de Bassoon pré-sináptico, enquanto que o efeito contrário é observado quando deletamos as proteínas Shank em fases tardias do desenvolvimento neuronal.

Além disto, foi também observado que a deleção dos genes SHANK2 e SHANK3 induzem apenas alterações morfológicas nas culturas primárias de hipocampus, sugerindo que alguns tipos de células poderão ser mais suscetíveis à perda de proteínas Shank do que outras.
Em suma, os nossos resultados fornecem evidências de que alterações no desenvolvimento neuronal e sináptico dependem (i) do tipo de células, (ii) da específica deleção das proteínas Shank e (iii) do estágio de neuro desenvolvimento. Os resultados apresentados são bastante importantes para uma melhor compreensão das alterações nos contactos sinápticos que ocorrem durante o processo de desenvolvimento dos modelos animais utilizados (murganhos com KO duplo e condicional de Shank2-3), as quais parecem ser dependentes da região cerebral.

Palavras-chave: ASD, Desenvolvimento neuronal, Plasticidade sináptica, Shank, Sinapse

Abbreviations

K^+ - potassium ion
Zn^{2+} - Zinc ion
βPIX - Rho guanine nucleotide exchange factor 7

AAV 2/5/9 – adeno-associated virus serotype 2/5/9
Abi-1 - abelson interactor 1
Abp1 - auxin binding protein 1
AMPA - α-amino-3-hydroxy-5-methyl-4-isoxazolepropionic acid
AMPAR - AMPA receptor
ANK - N-terminal ankyrin repeated
ASDs - autism spectrum disorders
ATG 5/7 - autophagy-related protein 5/7

bp - base pairs
BSA - bovine serum albumin

CA1 - Cornu Ammonis 1 region
CaMKII - calcium/calmodulin-dependent protein kinase type II

DIV - days *in vitro*

ERK - extracellular signal-regulated kinases

GFP - green fluorescent protein
GKAP - guanylate-kinase-associated protein
GluA1-3 - AMPA subunit

F-actin- actin filaments
Flx – floxed

HBSS - Hanks' Balanced Salt Solution
Homer1/3 - Homer protein homolog 1/3

IP3R - inositol triphosphate receptor
IQ - intelligence quotient
IRSp53 - insuline receptor substrate p53

KD - knock-down
KO - knock-out

LC3 - microtubule-associated protein 1 light chain 3
LTD - long-term depression

LTP - long-term potentiation

MAGUK - membrane-associated guanylate kinase
MAP2 - microtubule-associated protein 2
mEPSCs - miniature excitatory postsynaptic currents
mGluR1/5 - metabotropic glutamate receptor 1/5
MOI - multiplicity of infection
mRNA – menssager ribonucleic acid
mTOR - mammalian target of rapamycin

NMDA - N-methyl-D-aspartate
NMDAR - NMDA receptor
NR1/NR2A-B - NMDAR subunits
NRXN-NLGN – Neurexin- Neuroligin cell adhesion molecules

p62 - sequestosome-1
PDZ - PSD-95-Discs Large-zona occludens-1

PMS - Phelan-McDermid Syndrome
Pro - proline-rich region
ProSAP 1/2/3 - proline-rich synapse-associated protein 1/2/3
PSD-95 - postsynaptic density protein 95
PSD - postsynaptic density
PSVs - pre-synaptic vesicles

SAM - sterile alpha motif
SAPAPs - SAP90/PSD-95-Associated Proteins
SAP90 - Synapse-Associated Protein
SDS - sodium dodecyl sulfate
SH3 - Src Homology 3
Shank 1/2/3 - SH3 and multiple ankyrin repeat domains protein 1/2/3

TEM - transmission electron microscopy
VGLUT - vesicular glutamate transporter

1. Introduction

1. Introduction

1.1. The Shank protein family

Originally identified in 1998/1999 (1-4), the Shank family is constituted by: Shank1, Shank2 (also termed ProSAP1), and Shank3 (also termed ProSAP2) proteins. These large scaffold (3) and multi-domain proteins (2) form a highly ordered molecular complexes in the electron dense structure of excitatory glutamatergic synapses – the postsynaptic density (PSD) (5-7). Shank proteins interact with other scaffold and cytoskeletal proteins, and assemble glutamatergic receptors via conserved binding domains: N-terminal ankyrin repeated (ANK), Src Homology 3 (SH3), PSD-95-Discs Large-zona occludens-1 (PDZ), proline-rich region (Pro) and sterile alpha motif (SAM) at the C-Terminal (8) (Fig. 1). Consequently, these interactions make Shank proteins important mediators of synaptic development and function (2, 9-12).

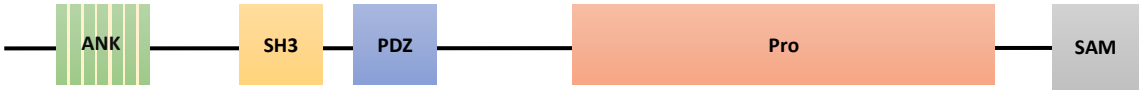

Fig. 1 | Overview of the Shank domain structure.

1.1.1. Expression pattern

Shank family members are encoded by SHANK1, SHANK2 and SHANK3 genes. In humans, the SHANK1 gene is located on chromosome 19q13.33, it has 24 exons and two different promoters that can lead to the expression of two currently known different protein isoforms: Shank1A and Shank1B (4, 13, 17). The SHANK2 gene is located on chromosome 11q13.3 and has 25 exons. It contains three alternative promoters that can generate four isoforms: Shank2A, Shank2B, Shank2C and Shank2E (1, 3). The SHANK3 gene, located on human chromosome 22q13.3, is composed by 22 exons and contains multiple intragenic promoters. These promoters together with alternative splicing code for an extensive number of mRNA and protein isoforms: Shank3A, Shank3B, Shank3C1, Shank3C3, Shank3C4, Shank3D1, Shank3D2, Shank3E1, Shank3E2 and Shank3F (14-16).

Expression of Shank proteins within the nervous system is detected in excitatory synapses (2-3), glial cells (17), olfactory cilia membranes (18), postsynaptic specializations of retinal (19) and skeletal neuromuscular junctions (20). However, Shank expression is not limited to the nervous system. In fact, Shank2 and Shank3 have also been identified in some non-neuronal tissue such as pancreas, pituitary, lung, liver, kidney, testis (17, 21-22), heart and spleen (4).

The expression of the different Shank proteins also seems to be different between different brain areas. Among the Shank family member, for example, Shank1 mRNA is the only family member that has been detected in the hypothalamus (8). Moreover, Shank1 is highly expressed in the cortex, hippocampus, thalamus, amygdala and cerebellar Purkinje cells (13, 23-24). Shank2 is strongly expressed in the cortex, hippocampus, thalamus and in cerebellar Purkinje cells (4, 24). The distribution of Shank3 mRNA is enriched in the cortex, hippocampus, striatum, thalamus and in cerebellar granule cells (24-26).

Interestingly, all the three family members show high expression levels within the hippocampus (27-29). Nevertheless, a very recent study revealed that Shanks are not uniformly expressed in

the mouse hippocampus: in fact, the three proteins are not found at VGLUT2- and VGLUT3-positive synapses, but co-localize only together with VGLUT1-positive stainings (30).
Additionally, the multiple Shank isoforms resulting from alternative splice variants display a brain region-specific expression pattern as well. Wang and collaborators (16) observed that Shank3 isoforms are expressed in a cell type, developmental and activity-dependent manner. Taken together, all these studies revealed that mRNA expression of Shank members results to be different, depending to brain areas and neuronal subpopulation.

1.1.2. Subcellular localization

The PSD is a highly organized protein complex constituted by receptors (including NMDAR, AMPAR and mGluRs), scaffold proteins (such as MAGUKs and Shank proteins), cell adhesion molecules (including neuroligins), signalling molecules (such as calcium/calmodulin-dependent protein kinase type II (CaMKII)) and cytoskeletal components. Together, they offer the essential support to the postsynaptic architecture and regulate the synaptic and/or neuronal physiology (31).
At the distal part of the PSD (about 120 nm away from the postsynaptic membrane) large platforms are found constituted by Shank proteins (14). They act as interface molecules between membrane receptors and cytoskeletal elements (6, 32), in order to control cytoskeletal dynamics and regulate activity-dependent neuronal signalling through trafficking, anchoring and clustering of glutamatergic receptors and cell adhesion molecules (33) (Fig. 2). This regulatory capability of synapses physiology depends on a complex domain composition of Shank family members - see **1.1. The Shank protein family** - that can be slightly different, depending on tissue, cell type and brain region, via alternative splicing events (4, 34).
The interaction between glutamate receptors and Shank proteins occurs mainly through the PDZ domain. NMDA receptors are stabilized at the postsynaptic membrane through GKAP/SAP90/PSD-95-Associated Proteins (SAPAPs), which are structurally supported by Shank PDZ domains. In contrast, the AMPA receptors are linked to the Shank complex via the interaction of PSD-95 with Stargazin or directly through the PDZ domain (35). The attachment of metabotropic glutamate receptors (mGluR) and inositol triphosphate receptor (IP3R) occurs through Homer proteins that bind to the Pro-rich domain of Shank proteins (9). On the other hand, the association of cytoskeletal elements with Shank proteins is realized via ankyrin repeats and/or the cortactin binding site (Cortactin, Abp1) , as well as with other motifs including the Pro-rich domain clusters (Abi-1, IRSp53) and the PDZ domain (βPIX, Fezzins) (36).
Although Shank members share a similar domain composition, they seem to have different interaction partner's preferences. In particular, Shank1 localization at synapses is mediated by the interaction between GKAPs proteins through the PDZ domain (10, 37). However, the C-terminal domain (including the SAM domains), which is involved in Shank multimerization via Zn^{2+} ions, is essential for Shank2 and Shank3 targeting and maintenance at synapses (38). As a consequence, different binding partners might control Shanks distribution at specific zones within the spine, in order to provide distinct molecular pathways.
Moreover, the variability of Shanks distribution in dendritic spines is also mediated by neuronal activity. At resting membrane potential, when the neurons show higher intracellular [K^+], Shank2 is concentrated at and near the PSD while Shank1 is, in addition, spread in the body of the spine. Following membrane depolarization with high K^+, the amount of Shank2 at PSD slightly increases, together with a pronounced, but transient increase of Shank1 (39). These

observations suggest that Shank1 is a dynamic element required for transient structural changes in the dendritic spine, while Shank2 is a fundamental element stabilized at PSD.
In light of these data, dendritically localized Shank mRNAs (13, 23, 40) and local translation close to spines (38) can serve as a local pool to provide fast structural synaptic changes after individual synapses stimulation.

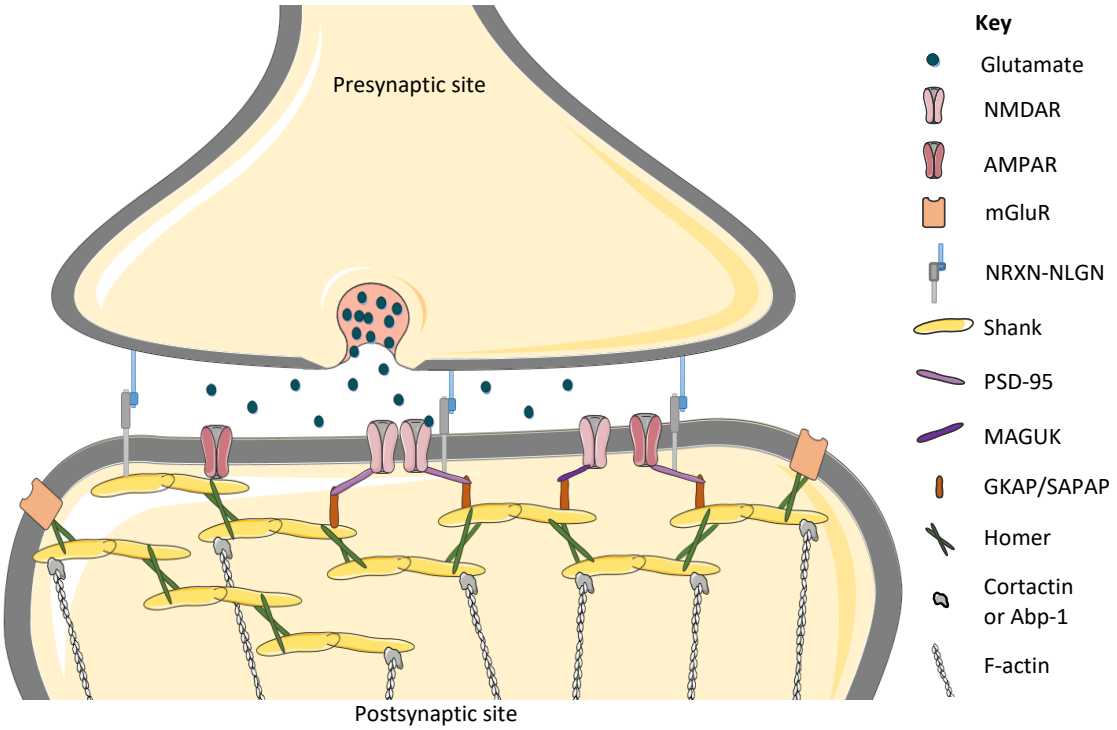

Fig. 2 | Functional overview of Shank proteins at excitatory synapses. Shank proteins form a structural network within the PSD through its interactions, and control a physical connection between glutamate receptors, cytoskeleton elements and components of several signalling cascades.

Nevertheless, there is evidence that the localization of Shanks within neurons is not limited to the PSD. Interestingly, recent studies highlighted that Shank3 can be translocated from synapses into the nucleus in a stimulus-specific manner to influence transcription (16, 41). Moreover, during development, Shanks also localize in other cell structures besides spines (1, 42), as will be discussed in the following section.

1.2. Shank proteins in neuronal development

Excitatory synapse formation is initiated through contact between a dendritic filopodium and an axon, followed by the recruitment of presynaptic pre-built transport vesicles to the active-zone containing important presynaptic proteins, such as Bassoon and Piccolo (43). The presynaptic differentiation precedes the dendritic spine specialization, which is mediated by constitutively alterations in the postsynaptic components (35, 44) and influenced by synaptic activity (45). Due to the roles of Shanks as major scaffolding proteins in the postsynaptic site, different studies have characterized their neuronal spatial distribution and relevance alongside with synaptogenesis (10, 46-48).
During neuronal development, Shank proteins are differentially incorporated into the PSD and their amount increases in parallel with synaptogenesis (3-4). In particular, Shank2 is one of the first molecules of the PSD binding to the sub-synaptic cytoskeleton even before PSD-95 and

NMDA receptors (3). In rat primary hippocampal neurons, when cells start to polarize and defining dendrites, as well as axons (3 days *in vitro* - DIV3), Shank2 is highly expressed. At this time-point, Shank2 appears to be equally distributed in the cell, but can be detected in dendritic clusters at DIV7, when excitatory synapses are already built (47). The appearance of Shank2 is followed by Shank3, with Shank1 being incorporated only later (49), suggesting that Shank2 and Shank3 are essential for the initial assembly and stability of immature synapses while Shank1 plays a major role in synapse maturation.

Shank1 overexpression in rat hippocampal neurons, for instance, induces dendritic spines enlargement through the recruitment of Homer1b protein (10). The complex formed between both molecules, interacts additionally with mGluR1/5 and IP3R, in order to control several signalling pathways (including ERK signal transduction pathway) underlying spine maturation (50). These effects were described as spine-specific, since they do not affect the spine number or the shape of the dendrites. In turn, Shank1 knock-down (KD) cause a reduction of spine size and excitatory synapse density (10).

The overexpression of Shank2 in rat hippocampal neurons leads to its accumulation at synapses and induces spine enlargement. In contrast, reduction of endogenous Shank2 decreases the excitatory spine volume and density, suggesting that Shank2 also plays an essential role in spine maturation (51).

The endogenous Shank3 levels are crucial for the maintenance of dendritic spines. Moreover, its overexpression orchestrates spine morphogenesis in mouse aspiny cerebellar neurons. Specifically, it induces increased synapses number and size, recruitment of glutamate receptors, as well as increased of amplitude, frequency and AMPA component of miniature excitatory postsynaptic currents (mEPSCs). On the other hand, Shank3 KD reduces spine density, but increases spine length (46).

In addition, there is growing evidence that Shank proteins are also required for the development of other neuronal cell compartments. During development, Shanks are found in neuronal growth cones of rat primary hippocampal neurons (1, 42), exhibiting different expression profiles (48). In later stages of development, Shanks are also expressed in axons of polarized neurons and are localized in axon terminals, where they co-localize with the presynaptic proteins Bassoon and VGluT1 (48)

Intriguingly, Shank3 KD leads to an upregulation of the NMDAR subunit NR1, suggesting that Shank3 also modulates NMDAR levels presynaptically (48).

Taken together, these results indicate that endogenous levels of Shank proteins play a central role in: induction, maturation and stabilization of dendritic spines; synaptic junction organization; axonal outgrowth; and also in presynaptic terminal development and function. Therefore, is not surprising that disruption of SHANK human genes can lead to severe synaptic and circuitry defects that are underlying neurodevelopmental diseases such as autism spectrum disorders (ASDs) - see **1.4. The genetic linkage between SHANK mutations and ASD**.

1.3. Synaptic turnover in neuronal development

Despite the fact that synapses display a high molecular complexity, their structure and composition undergo continuous remodelling during development (31). In early stages of neuronal development, there is an overabundance of synapse formation followed by a maturation phase, which is characterized by elimination/pruning of redundant connections.

Both, synaptic gain and elimination are under balance during neuronal development and are key events in the establishment of functional neuronal circuits (52).

In parallel with those structural changes, the PSD protein composition is in constant flux as well. Proteins have a finite lifetime and their synthesis and degradation are required to maintain a continuous level of proteins at synapses (53). Nevertheless, protein turnover in not only important to maintain a proper protein concentration, but it also allows synaptic changes and viability (54).

PSD composition is modified on a timescale of hours to days under resting condition (55-56) and shows larger changes in response to synaptic activity (57). Activity-dependent modifications of PSD include redistribution of specific proteins, to and away from the PSD (such as CaMKIIα and scaffold proteins), as well as insertion and removal of glutamate receptors (such as AMPARs) (39, 57-58). Together, these changes mediate strengthening and weakening of synaptic transmission produced by long-term potentiation (LTP) and long-term depression (LTD), respectively (59).

The abundance of PSD components is additionally regulated by local protein translation (60) and by the ubiquitin-proteasome system for protein degradation (61). The mammalian target of rapamycin (mTOR) signalling pathway plays an important role in mRNA translation through controlling activity of translation factors (62). Several components of this pathway, including mTOR kinase, can been found in dendrites, at presynaptic bouton, and at postsynaptic site overlapping with PSD-95 (63), suggesting that mTOR can regulate the protein synthesis at synapses. On the other hand, mTOR activation inhibits autophagy (64), a self-digestive process responsible of maintaining essential activity levels in resposnse to stress situations, such as nutrient starvation (65). Together with the ubiquitin-proteasome system, autophagy constitutes the major pathway for protein degradation (52).

The ubiquitin-proteasome system has been described as crucial in regulation of synaptic growth through controlling the turnover of short-lived cytosolic proteins (66-67) such as GKAP and Shank scaffolds (61). In contrast, autophagy is responsible to sequester long-lived proteins and damaged organelles into a double-membrane autophagosome which fuse with lysosomes to degrade the cargo (52). Nevertheless, recent studies have emphasized the importance of autophagy during synaptogenesis. Studies using transmission electron microscopy (TEM) highlighted the presence of autophagosomes in the synaptic terminals of cultured hippocampal neurons (68). Moreover, the downregulation of autophagy-related protein 7 (ATG7), an essential molecule for the isolation of the membranes necessary for autophagosomes formation (69), leads to an increase of spine number during the mature stage of cultured hippocampal neurons development (DIV21-28). However, the synaptogenesis (DIV6-21) of hippocampal neurons deficient in ATG7 was not affected (70). These findings indicate that the impairment of autophagy exerts no effect on spine formation but reduces the pruning of redundant synapses, leading to an excessive spine density.

Proper elimination of synapses provides selection and maturation of neural circuits, while abnormal synaptic pruning has been associated to neurodevelopmental disorders, including ASD (52). Indeed, some patients with ASD show increased spine density in frontal, temporal and parietal lobes. These deficits are associated with reduced cognitive function (71) and are mainly caused by hyperactivation of the mTOR signalling pathway and autophagy impairment (70). Therefore, synaptic protein synthesis and degradation must be in equilibrium to support a correct synaptic development and plasticity.

1.4. The genetic linkage between SHANK mutations and ASD

Autism spectrum disorder (ASD) comprises multiple neurodevelopmental disorders characterized by impairments in social interaction and communication, and by unusual repetitive behaviours. These symptoms manifest in early childhood and currently affect about 1% of the population (data from public–private research program EU-AIMS, 2016). These patients can also show comorbidities as cognitive defects, hyperactivity, anxiety, hypotonia, epilepsy and sleep disorders making ASD highly heterogeneous (14, 72-73).

Despite the causes of ASD remain largely unknown (74), several studies performed in families with autism history have highlighted a strong genetic contribution to these diseases (75). Among the significant number of genes that have been associated with ASD (76) a large portion encode for proteins required for the proper formation, maintenance and functionality of synaptic connections (77-79), such as SHANK3, neuroligin 3, neuroligin 4 and neurexin 1 (14, 13).

Shanks were initially associated with ASD, when the disruption of SHANK3 gene was recognized as the major cause of the symptoms of Phelan-McDermid Syndrome (PMS) (80). This syndromic form of autism is characterized by significant expressive language delay, intellectual disability, neonatal hypotonia, minor craniofacial dysmorphisms, increased tolerance to pain and epilepsy (80-81). In addition to these symptoms, more than 50% of the patients with PMS show behavioural deficits (82). Nevertheless, mutations in SHANK3 gene are not restricted to patients with PMS. Microdeletions, nonsense mutations, breakpoints and missense mutations in SHANK3 gene have also been detected in patients with other forms of autism (14).

The special interest in the link of SHANK mutations to ASD that has emerged revealed that SHANK1 (83) and SHANK2 mutations (84-85) are also detected in individuals with ASD. A meta-analysis study has shown that approximately 1% of all the patients with ASD have mutations or disruptions in the SHANK gene family with an incidence of 0.04%, 0.17% and 0.69% in SHANK1, SHANK2 or SHANK3, respectively (86). Additionally, the same study demonstrated SHANK mutations are detected in the whole spectrum of autism with a degree of cognitive impairment (in the following order: SHANK3>SHANK2>SHANK1). Indeed, SHANK3 mutations are highly penetrant and are found in patients with moderate to severe intellectual disability. In comparison with SHANK3 mutations, SHANK2 mutations lead to mild intellectual disability, while patients with SHANK1 mutations have a normal intelligence quotient (IQ).

Overall, these data provide the evidence that SHANK family of genes disruption is remarkably associated with ASD. However, the exact role of the distinct Shank proteins in physiological conditions, as well as, how they are disrupted in ASD still unclear. Therefore, *in vitro* and *in vivo* models are indispensable to achieve these questions.

1.5. The neurological defects in *Shank*-mutant mouse models

Given the high relevance of SHANK genes in ASD, different mouse models carrying mutations in the SHANK gene family have been generated. In line with the human genetic data described above - **1.4. The genetic linkage between SHANK mutations and ASD** - these mouse lines show variable behavioural, functional and molecular phenotypes depending on which SHANK gene has been manipulated.

The disruption of the SHANK3 gene in nine of the thirteen *Shank3*-mutant mouse lines that have been reported so far, results in severe phenotypes, such as altered social behaviour and repetitive behaviours (over-grooming). Further studies revealed that ultrasonic vocalizations

and cognitive abilities were differentially affected in the distinct *Shank3*-mutant mouse lines evaluated due to the variability of mutation nature and isoforms affected in each line (14).

Similarly to *Shank3*-mutant animals, the two *Shank2*-mutant mouse lines reported so far (87-88) also show behavioural deficits, such as decreased social interaction and altered ultrasonic vocalization. However, excessive self-grooming is only present in the mouse line lacking the exon 17 (where the PDZ domain is localized) (88) while the mouse lacking the exons 16 and 17 shows reduced spatial learning and memory (87).

To date, only one *Shank1*-mutant mouse line has been reported (89-91). The lack of all the SHANK1 isoforms leads to impairments in motor coordination, in contextual fear memory and long-term memory. In contrast with *Shank3*- and *Shank2*-mutant mouse lines, repetitive self-grooming was not observed in this model.

In parallel to these behavioural effects, all *Shank*-mutant mouse lines exhibit electrophysiological defects. Due to the strong association between cortico-striatal circuitry dysfunction and repetitive/compulsive behaviours (24, 92-93), some *Shank3*-mutant mouse lines generated (24, 26, 94-96) have been particularly studied for electro physiological perturbations in cortico-striatal synapses. In adulthood, these mice show reduced cortico-striatal connectivity and decreased mEPSC frequency in striatal neurons (24, 26, 94-95). However, during early development the *Shank3*-mutant mice exhibit opposite alterations (enhanced cortico-striatal connectivity and increased striatal mEPSC frequency), which are triggered by cortical hyperactivity (96). Overall, these results indicate that the SHANK3 disruption leads to early imbalances in cortical function, which modify the normal course of cortico-striatal circuit development.

The lack of SHANK2 gene leads to changes in NMDAR- mediated excitatory synaptic transmission and, as consequence, the *Shank2*-mutant mouse lines show altered glutamatergic neurotransmission (87-88). On the other hand, the *Shank1*-mutant mouse line displays reduced mEPSC frequency in hippocampal CA1 pyramidal neurons (89) and in parvalbumin-positive CA1 interneurons (97), suggesting that Shank1 can regulates excitatory and inhibitory synaptic transmission.

Considering the importance of Shank proteins as regulators of the PSD composition, a few studies have analysed molecular and morphological changes at the synapse, which might lead to the behavioural and electrophysiological abnormalities observed in adult *Shank*-mutant mice. The levels of two major Shank-interacting proteins (Homer and SAPAP) have been found reduced at the PSDs of the cortex (98) and striatum (24, 94) of *Shank3*-mutant mice, as well as in the hippocampus *of Shank1*-mutant mice (92). Interestingly, no significant changes were found in the levels of these scaffold proteins in the synaptosomal preparations from the cortex and cerebellum of *Shank3*-mutant mice (94), suggesting that some brain regions might be more susceptible than others to SHANK gene absence.

The total levels of NR1 was found upregulated in the whole brain lysates of *Shank2*-mutant mouse lines. However, no changes in synaptic scaffolds levels (such as Homer and PSD-95) were reported in *Shank2*-mutant animals (87).

Schmeisser and collaborators (88) performed an extensive study on the expression of several glutamate receptor subunits in different brain regions of *Shank2*- and *Shank3*-mutant mice lines. The expression of NR1 and NR2B (hippocampus), as well as NR1, NR2A and GluA2 (striatum) were found to be upregulated in synaptosomal fractions isolated from *Shank2*-mutant mice. In contrast, the *Shank3*-mutant animals only exhibit an increase of NR2B protein levels at the PSDs

of the hippocampus. No significant differences were found in the expression of NMDAR and AMPAR subunits in the cortex from both mouse lines. Additionally to these changes, the Shank3 protein level at synapses was increased in the striatum of *Shank2*-mutant mice, while the Shank2 protein level at synapses was upregulated in the striatum of *Shank3*-mutant mice (88). Since no significant changes in these proteins were observed in others brain regions, this last observation suggests that a compensatory mechanism between Shank2 and Shank3 proteins might take place in a brain–region-specific manner.

Morphologically, *Shank*-mutant mice show also alterations regarding the PSD size and dendritic spine structure. In hippocampal neurons of *Shank1*-mutant mice the dendritic spines are reduced and the PSDs thinner (89). Similar structural changes have been reported in *Shank2*-mutant mouse line by Schmeisser and collaborators (88). The data obtained from *Shank3*-mutant mice studies demonstrate that dendritic spines are longer and less dense in hippocampus (98) and in striatum (24). Moreover, the same studies revealed that PSD thickness is reduced in striatal neurons but not in hippocampal neurons. For further information on the synaptic molecular and structural analysis in *Shank*-mutant mice, see Table 1, 2 and 3.

Taken together, these findings indicate that the dysregulation of SHANK genes expression in *Shank*-mutant mice triggers abnormal synaptic composition and function, as well as, similar comorbidities described in patients with ASD. Additionally, different molecular and physiological phenotypes are observed in distinct brain regions, depending on which SHANK gene is mutated. Therefore, each Shank mutation might affect specific brain circuits and lead to a defined ASD phenotype.

Since ASDs comprises neurodevelopment disorders and Shank proteins display a fundamental role in the organization of the PSD composition and structure, one question that remains to be explained is whether there is a critical time window during which SHANK genes expression is crucial for the development. A recent study generated a *Shank3*-mutant mouse line carrying a FLExed PDZ domain inverted (94). When combined with Cre-recombinase activity the PDZ domain is reoriented to the original position leading to SHANK3 WT gene expression. Therefore, those mice are born as *Shank3*-KO and exhibit changes in the PSD composition of striatal neurons, neurotransmission abnormalities and autistic-like behaviours. Surprisingly, the establishment of SHANK3 expression in adulthood efficiently restored the proper PSD levels and the neurotransmission in the striatum neurons, rescued the altered social behaviour and reduced the over-grooming. However, other autistic-like behaviours (such as anxiety and motor coordination) were not rescued by SHANK3 expression after development, suggesting that appropriate Shank protein levels during neuronal development are essential for the normal course of neuronal circuits.

Table 1 | Synaptic molecular and morphological analysis in Shank3-mutant mice

***Shank3*-mutant mouse lines**							
Protein domain affected	**Exon mutated/ Deleted**	**Molecular Changes**					**Refs**
		Whole brain	**Hippocampus**	**Cortex**	**Striatum**	**Cerebellum**	
ANK	Δex4-9	N/I	↓ NR1 clusters	N/I	N/I	N/I	99
		N/I	N/I	Homer1 b/c, ↓ GKAP, GluA1, NR2B levels	N/I	N/I	98
		N/I	N/I	N/I	Homer1, PSD-95, ↓ GluA2, GluA3 levels	N/I	100
SH3	Δex11	N/I	↑ NR2B levels NR1, NR2A, GluA1-3 levels	NR1, NR2A-B, GluA1-3 levels	↑ Shank2 levels NR1, NR2A-B, GluA1-3 levels	N/I	88
		N/I	Homer1, mGluR5 levels	↓ Homer1, mGluR5 levels	↓ Homer1 levels mGluR5 levels	N/I	101
PDZ	Δex13-16	N/I	N/I	N/I	Homer1, SAPAP3, ↓ PSD-93, GluA2, NR2A-B levels PSD-95, NR1, GluA1 levels	N/I	24
	FLEX-Δex13-16	N/I	N/I	↑ Shank2 levels Shank1, Homer1, PSD-95, SAPAP3, NR1, NR2A-B GluA1-2 levels	Homer1, SAPAP3, ↓ GluA2, NR2A-B levels Shank1-2, PSD-95, NR1, GluA1, mGluR5 levels	↓ GluA1 levels Shank1-2, Homer3, PSD-95, SAPAP3, NR1, NR2A-B GluA2 levels	94
Pro	Δex21	N/I	↑ mGluR5 levels SAPAP3, PSD-95, NR1, NR2A-B GluA1-2 levels	N/I	N/I	N/I	102
	InsG3680-ex21	N/I	N/I	↓ Homer, PSD-95, PSD-93 levels SAPAP3, NR2A-B, GluA1-2, mGluR5 levels	Homer1, SAPAP3, PSD-95, SynGAP1, ↓ GluA2, GluA5, NR1, NR2A-B, mGluR5 levels SAPAP3, GluA1 levels	N/I	95
All	Δex4-22	N/I	↓ Homer1 b/c-3, GluA2 levels mGluR5 levels	N/I	↓ Homer1 b/c-2, SAPAP3 levels mGluR5 levels	N/I	26
Protein domain affected	**Exon mutated/ deleted**	**Morphological Changes**					**Refs**
		Whole brain	**Hippocampus**	**Cortex**	**Striatum**	**Cerebellum**	
ANK	Δex4-9	N/I	Deficits in spine remodelling	N/I	N/I	N/I	99
		N/I	↓ Spine density	N/I	N/I	N/I	98
		N/I					100
SH3	Δex11	N/I					88
		N/I					101
PDZ	Δex13-16	N/I	N/I	N/I	Neuronal hypertrophy, ↓ Spine density, PSD thickness	N/I	24
	FLEX-Δex13-16	N/I	N/I	N/I	↓ Spine density	N/I	94
Pro	Δex21	N/I	Dendritic complexity, spine density	N/I	N/I	N/I	102
	InsG3680-ex21	N/I	↓ Spine density	N/I	N/I	N/I	95
All	Δex4-22	N/I	Spine density	N/I	↓ Spine density	N/I	26

Upregulated; downregulated; nonsignificant changes.

Table 2 | Synaptic molecular and morphological analysis in Shank2-mutant mice

***Shank2*-mutant mouse lines**							
Protein domain affected	**Exon mutated/ deleted**	**Molecular Changes**					**Refs**
		Whole brain	**Hippocampus**	**Cortex**	**Striatum**	**Cerebellum**	
PDZ	Δex17	N/I	↑ NR1, NR2B levels Shank3, NR2A, GluA1-3 levels	Shank3, NR1, NR2A-B, GluA1-3 levels	↑ Shank3, NR1, NR2A levels NR2B, GluA1, GluA3 levels	N/I	88
	Δex16-17	↑ NR1 levels Homer1, PSD-95, GKAP, NR2A, GluA2, mGluR1, mGluR5 levels	N/I	N/I	N/I	N/I	87
Protein domain affected	**Exon mutated/ deleted**	**Morphological Changes**					**Refs**
		Whole brain	**Hippocampus**	**Cortex**	**Striatum**	**Cerebellum**	
PDZ	Δex17	N/I	↓ Spine density PSD thickness	N/I	N/I	N/I	88
	Δex16-17	N/I	Spine density, PSD thickness	N/I	N/I	N/I	87

Upregulated; downregulated; nonsignificant changes.

Table 3 | Synaptic molecular and morphological analysis in *Shank1*-mutant mice

***Shank1*-mutant mouse line**							
Protein domain affected	**Exon mutated/ deleted**	**Molecular Changes**					**Refs**
		Whole brain	**Hippocampus**	**Cortex**	**Striatum**	**Cerebellum**	
PDZ	Δex14-15	N/I	↓ SAPAP, Homer1 levels PSD-95, NR1, GluA1-2, mGluR5 levels	N/I	N/I	N/I	89
Protein domain affected	**Exon mutated/ deleted**	**Morphological Changes**					**Refs**
		Whole brain	**Hippocampus**	**Cortex**	**Striatum**	**Cerebellum**	
PDZ	Δex14-15	N/I	↓ Spine density, spine size, PSD thickness	N/I	N/I	N/I	89

Upregulated; downregulated; nonsignificant changes.

2. Aim

2. Aim

ASD is a neurodevelopmental disorder characterized by several and different features as impaired communication skills, stereotyped movements, reduced interests and attention, and difficulties in social interaction (14, 72-73). Although this broad range of symptoms is seemingly unrelated, several recent publications have highlighted important roles of specific brain regions (such as striatum, hippocampus and cortex) in controlling and coordinating autism-associated behaviours (24, 88, 94). Moreover, the consideration that several autism genes are ubiquitously expressed in the whole brain supports the idea that specific neuronal circuitry and cell types are more likely to contribute in ASD onset. In addition, different ASD risk genes encode for synaptic proteins playing crucial roles in the regulation of synaptic plasticity and pruning during the neurodevelopmental timeframe – see **1. Introduction**.
Given these considerations, the goal of our study is to elucidate the role played by two ASD-related scaffold proteins, Shank2 and Shank3, during neuronal development. In particular, we aimed to answer two major questions to contribute in clarifying the still poorly understood connections between synaptic impairment and Autism Spectrum Disorders (ASDs):

- Synaptic plasticity modulation through *non-conventional* induction: do Shanks undergo changes under stress conditions and altered neuronal activity?
- Time- and cell type specific depletion of Shank2 and Shank3: how different neuronal populations develop in absence of the two major scaffold proteins?

Emerging lines of evidence highlight the involvement of autophagy in synaptic structural and molecular changes. For instance, autophagy impairment has been associated to autism via a failure of autophagy-mediated pruning of synapses during neuronal development (70). Moreover, a recent study revealed that this degradative mechanism seems to be negatively modulated by a presynaptic protein, Bassoon, to maintain the synapse proteostasis (103). Given these interesting findings, we decided to induce autophagy to investigate synaptic dynamics that might occur, in particular on Shank family elements. For this purpose it was important to preserve the synaptic ultrastructural morphology to achieve a better evaluation of synaptic changes. Therefore, we used high pressure freezing as cryo-fixation method for TEM analysis, which provides a fast immobilization of macromolecular components under high pressure and reduces the undesired effects produced by crystallisation (104).
To address the second question of our project we generated a new *Shank2 Shank3* conditional KO mouse line – *Shank2*$^{flx/flx}$ *Shank3*$^{flx/flx}$ – through the cross breeding of *Shank2*- and *Shank3*-mutated mice previously described by Schmeisser and collaborators (88). Since both SHANK2 and SHANK3 genes are targeted, this animal model might provide new insights to clarify the mechanistic links between synaptic abnormalities and ASD-related genes. Moreover, it enables the temporal control of SHANK2 and SHANK3 genes disruption, which may help us to investigate the impact of Shank2 and Shank3 protein loss at different stages of neuronal development. To follow the neuronal development events and achieve a high resolution of synaptic features under Shank2 and Shank3 deficiency we established primary hippocampal and cortical neuronal cells derived from *Shank2*$^{flx/flx}$ *Shank3*$^{flx/flx}$ embryonic mice. Therefore, this system could further help in understanding the heterogeneous vulnerability of different cellular populations characterizing ASDs.

3. Materials and Methods

3. Materials and Methods

3.1. Antibodies

Table 4 | Information of primary and secondary antibodies.

Antibody	Specie	Production	Dilution		Company
			ICC	WB	
Primary Antibodies					
β-Actin	Mouse	Monoclonal	-	1:250.000	Sigma-Aldrich
Bassoon	Mouse	Monoclonal	1:1000	-	Enzo
Cre-Recombinase	Rabbit	Monoclonal	1:500	-	Cell Signaling Technology
Gephyrin	Mouse	Monoclonal	1:500	-	Synaptic Systems
GFP	Mouse	Monoclonal	1:2000	-	Clontech
Homer 1	Guinea pig	Polyclonal	1:500	-	Synaptic Systems
LC3	Rabbit	Monoclonal	-	1:1000	Cell Signaling Technology
MAP2	Guinea pig	Polyclonal	1:500	-	Synaptic Systems
MAP2	Chicken	Polyclonal	1:750	-	EnCor Biotechnology
NR1	Rabbit	Polyclonal	1:400	-	Sigma-Aldrich
Shank2	Rabbit	Polyclonal	1:500	-	Self-made
Shank3	Rabbit	Polyclonal	1:500	-	Self-made
p62	Mouse	Monoclonal	1:500	1:1000	Abcam
Secondary Antibodies					
Alexa 488	Anti-rabbit Anti-mouse Anti-guinea pig Anti-chicken	Polyclonal	1:1000	-	Molecular Probes
Alexa 568					
Alexa 647					
AMCA	Anti-chicken	Polyclonal	1:50	-	Jackson ImmunoResearch
	Anti-guinea pig				
HRP	Anti-mouse	Polyclonal	-	1:1000	Dako
	Anti-rabbit			1:3000	

3.2. Cre-recombinase delivering strategies

For genetic manipulation two methods were tested: viral transduction and TAT peptide-mediated cellular delivery (Table 5). Viral transduction using AAV9-Syn-Cre-GFP was defined as the best method to use. For further details please see Fig. 7B – **4. Results**.

Table 5 | List of gene delivery methods tested.

Cre-Expressing Virus	MOI Tested	Company
AAV2-CMV-Cre-GFP	100.000; 150.000; 200.000	SignaGen
AAV5-CMV-Cre-GFP	100.000; 150.000; 200.000	Viral Vectors
AAV9-Syn-Cre-GFP	100.000; 150.000; 200.000	SignaGen
CMV-Cre-GFP-Lentivirus	1; 2.5; 5; 10; 15	Cellomics Technology
TAT-Peptide	**Concentrations Tested**	**Company**
TAT-Cre Recombinase	0.25 µM; 0.5 µM; 0.75 µM; 1 µM; 2 µM	Milipore

3.3. Primary neuronal cultures

3.3.1 Primary mouse hippocampal and cortical neuronal cultures

Primary neuronal cultures were prepared from embryonic hippocampal and frontal cortical tissue. Preparations of *Shank2 Shank3* conditional KO (*Shank2*$^{flx/flx}$ *Shank3*$^{flx/flx}$) mouse embryos were carried out at gestational day 17 or 18 (E17-18). Dissection procedures were performed into Hanks' Balanced Salt Solution w/ $CaCl_2$ w/ $MgCl_2$ (HBSS, Gibco Life Technologies) at 4ºC. After dissection, the tissues were separately incubated for 15 min with 0.25% trypsin-EDTA (1x) (Gibco Life Technologies) at 37ºC and 5% CO_2 (the tubes were gently inverted every 5 min to facilitate the trypsinization). The tissues were washed once with Dulbecco's Modified Eagle Medium high glucose (4.5 g/L) (DMEM, Gibco Life Technologies), supplemented with 10% fetal bovine serum (FBS, Sigma), 1% penicillin/streptomycin (P/S, Gibco Invitrogen) and 1% L-Glutamine (100x) (L-Glu, Gibco Life Technologies). Afterwards, were mechanically dissociated in Neurobasal Medium (1x) (Gibco Life Technologies) supplemented with 10% horse serum (HS, Sigma-Aldrich), 1% P/S, 1% L-Glu, 2% B27 (50x) (Gibco Life Technologies) and Deoxyribonuclease I (Invitrogen Life Technologies). The remaining tissue was separated from supernatant with a 100 µm filter. The cells were counted and plated with Neurobasal Medium, supplemented with 10% HS, 1% P/S, 1% L-Glu and 2% B27, in 24-well plate ($4x10^4$ cells/well) containing glass coverslips previous coated with 0.1% gelatin type A (Sigma-Aldrich) for 48h followed by 24h in Poly-L-lysine hydrobromide (PLL, Sigma-Aldrich).

After 3h and 24h of cell plating, half of the old media was replaced by Neurobasal Medium, supplemented with 10% HS, 1% P/S, 1% L-Glu and 2% B27. Cell cultures were maintained in a humidified incubator at 37ºC and 5% CO_2, for up to 20 days *in vitro* (DIV) and fed twice per week

with Neurobasal Medium, supplemented with 10% HS, 1% P/S, 1% L-Glu and 2% B27 during the early stages of neuronal development and with Neurobasal Medium, supplemented 1% P/S, 1% L-Glu and 4% B27 during neuronal maturation phase.

3.3.2. Primary rat hippocampal neuronal cultures

Rat hippocampal neurons were prepared from rat embryos (Sprague-Dawley rats, Janvier Laboratories) at E17-18. All the dissection and dissociation procedures were performed as described above - **3.3.1. Primary mouse hippocampal and cortical neuronal cultures** – with minor modifications: the medium used for cell dissociation was not supplemented with 10% HS and Deoxyribonuclease I. After counting, the cells were plated with Neurobasal Medium, supplemented with 10% HS, 1% P/S, 1% L-Glu and 2% B27, in 10-cm-diameter petri dishes ($3x10^6$ cells/dish) previous coated with PLL for 1h (immunoblotting studies) or in 24-well plate ($3x10^4$ cells/well) containing glass coverslips coated with PLL for 24h (immunocytochemistry analysis) or sapphire discs coated with carbon using a BAF 300 electron beam evaporation device (Balzers) followed by 24h in PLL (transmission electron microscopy - TEM - purposes).
After 3h and 24h of cell plating, half of the old media was replaced by fresh Neurobasal Medium. Cell cultures were maintained in a humidified incubator at 37ºC and 5% CO_2, for up to DIV14 and fed once per week with Neurobasal Medium.
For starvation experiments, DIV14 neurons were incubated with HBSS at 37ºC in 5% CO_2 for 5h. Control cultures were kept in Neurobasal Medium. After the incubation period, the cells were proceed for immunoblotting, immunocytochemistry or TEM studies.

3.4. *Shank2*$^{flx/flx}$ *Shank3*$^{flx/flx}$ mouse genotyping

For genotyping, a portion of the tail was taken from the pregnant mouse during dissection for primary neurons. The tail was frozen at -80ºC for 15 to 30 min before being incubated with lysis buffer (1 mM Tris, pH 8.0, 100 mM EDTA, pH 8.0, 0.5% SDS, 0.5 mg/mL Proteinase K, 0.2 mg/mL RNAse) for 1h at 56ºC in shaking. Afterwards, the sample was centrifuged at 13000 rpm at RT, for 10 min. The supernatant was collected in a new tube and incubated with isopropanol at RT for 10 min. After incubation, the centrifuge step was repeated twice and the resultant pellet was washed with ice-cold 70% ethanol between centrifugations, before drying. Finally, Tris-EDTA (TE) buffer (10 mM Tris-HCl, pH 7.4, 1 mM EDTA, pH 8.0) was added before polymerase chain reaction (PCR) reaction.
To amplify the sequence of SHANK2 allele, the forward primer 5' TCCGCAGA CCACTTTATTCC 3' and the reverse primer 5' GGCCAAGTTCCATGTATGCT 3' to produce a band of 613 base pairs (bp) for WT allele and 855 bp for SHANK2 flx allele were used. For the SHANK3 allele, PCR were performed using the forward primer 5' GTCTCTGTGGTTGGGGTGTC 3' and the reverse primer 5' CAGTG AAGAAGCCCCAGAAG 3' to produce a band of 250 bp for WT allele and 400 bp for SHANK3 flx allele. The primers used were produced by Eurofins Genomics.
The PCR reactions were performed in PCR SuperMix solution (Invitrogen Life Technologies) using the thermal cycling conditions described in Table 6. After amplification, the DNA fragments were isolated by DNA electrophoresis in a 1.5% agarose gel in 1x Tris-acetate-EDTA (TAE) buffer (40 mM Tris, pH 7.6, 20 mM acetic acid, 1 mM EDTA), carried out at 110V for 30 min in 1x TAE buffer. The DNA samples were loaded with 0.05 µL/mL of RedSafe solution (20,000x) (DNA-binding dye,

iNtRON Biothecnology), alongside with a DNA ladder (Invitrogen Life Technologies). The DNA fragments were visualized using an ultraviolet (UV) transilluminator equipped with a camera.

Table 6 | PCR conditions for Shank2$^{flx/flx}$ Shank3$^{flx/flx}$ mouse genotyping.

Steps	PCR		
	Nº of cycles	Temperature	Duration (min)
Initialization	1X	95ºC	03:00
Denaturation	36x	95ºC	00:30
Annealing		60ºC	01:00
Extension		72ºC	01:30
Elongation	1x	72ºC	10:00

3.5. Primary Neuronal Transduction by Adeno-Associated Virus Serotype 9

Primary mouse neurons were infected at early stages of development (DIV3 and DIV7) and in mature stage (DIV14) with AAV9-Syn-Cre-GFP virus diluted in Neurobasal Medium, supplemented with 1% P/S, 1% L-Glu and 2% B27, using a multiplicity of infection (MOI) of 100 000 viral genomes per cell. Uninfected cells used as control were kept in Neurobasal Medium. After 3 days of infection, half of the virus-containing medium was replaced with fresh Neurobasal Medium. At DIV20, the cells were processed for immunocytochemistry.

3.6. Immunocytochemistry, Imaging and Quantitative Analysis

Cells grown in glass coverslips were washed once with $CaCl_2$- and $MgCl_2$- free Dulbecco's Balanced Salt Solution (DPBS, Gibco Life Technologies) before being fixed and permeabilized with ice-cold methanol for 5 min at -20ºC, and blocked with blocking solution [10% goat serum (GS, Milipore) in DPBS and 0.2% Triton X-100 (Roche)] for 90 min at RT. Neurons were then incubated with the primary antibodies diluted in blocking solution for 48h at 4ºC. After incubation with primary antibodies, cells were washed 3 times with DPBS for 20 min. Afterwards, cells were incubated with the secondary fluorescent antibodies diluted in DPBS for 90 min at RT, at dark. Finally, cells were washed with DPBS 3 times for 20 min, and mounted on glass slides with Aqueous Mounting Medium (VectaMount, Vector Laboratories). After drying, glass slides were stored at 4°C.

Imaging was performed on a Zeiss Imager Z1 microscope, using a Plan-Neofluar 63x/1.25 oil objective. Identical settings were applied to each set of markers in control and treatment conditions, between experiments.

For quantification, the image analysis software ImageJ was used applying an equal threshold to each set of markers between independent experiments.

In Shank2 and Shank3 knockout studies, transduced neurons were identified by intrinsic GFP-positive signals at nuclei in cells positively immunostained against the neuronal marker MAP2.

For pre- and postsynaptic markers signal quantification, dendrites were randomly selected and measured through the MAP2 staining. Three dendrites of 30 µm were analysed per cell. Results are given as relative number of synaptic clusters per 30 µm.
For p62 signal quantification, neuronal cell bodies were randomly selected through the MAP2 staining as well.
For Sholl analysis, only neurons with clearly identifiable dendrites and with relative non-overlap by surrounding neurons were analysed. The selection was performed through the MAP2 staining, using a Plan-Neofluar 20x/0.50. The entire neuronal arborization of each neuron was reconstructed and analysed using the image analysis software Imaris (Bitplane).
Three independent experiments were performed, and at least 10 cells per condition were analysed.
For displaying images between experiments, images were manipulated post-acquisition applying the same parameters.

3.7. Transmission Electron Microscopy (TEM), Imaging and Quantitative Analysis

The sapphire discs were removed from the 24-well plate and dipped once in 95% 1-hexadecene (Sigma-Aldrich). Two sapphire discs oriented face-to-face and separated by a gold ring (3.05 mm diameter, Plano) were mounted into a holder (Engineering Office, M. Wohlwend) and placed into a Wohlwend HPF Compact 01 high-pressure freezer (Engineering Office, M. Wohlwend). The samples were frozen with liquid nitrogen at a pressure of 2100 bar. After high-pressure freezing, the sapphire discs were separately incubated in 1.5 mL precooled (−87°C) sample tubes filled with 1 mL freeze substitution solution (0.2% osmium tetroxide, 0.1% uranyl acetate, 5% dH_2O in acetone). After the tube had been warmed up to 0°C the samples were washed 3 times with 1 mL 100% acetone and transferred into a clean tube containing 0.25 mL 100% epoxy resin and incubated for 24h at 60°C to polymerize the resin. The samples were stored at RT after polymerization. For specimen preparation, 70-100 nm-thick sections were cut off from the epoxy resin block parallel to the plane of the sapphire disc with an Ultracut UCT ultramicrotome (Leica) equipped with a diamond knife (Diatome). After mounting the slice onto a 300 mesh copper grid, sections were stained with 0.3% lead citrate for 1 min, washed with dH_2O and dried at RT.
The samples were examined with a Jeol JEM 1400 (Jeol) transmission electron microscope at 100 kV. Images were randomly recorded with an exposure time of 14000 milliseconds and saved with a resolution of 4 megapixels (2,048 × 2,048). For our purposes, a magnification of 80.000x was chosen. Only artifact-free synapses, with clearly identifiable presynaptic and postsynaptic terminals, synaptic clefts and PSD were selected for analysis. The PSD length and thickness as well as the width of synaptic cleft were measured using ImageJ software. To calculate the PSD volume, was used the following formula: PSD volume = $(\text{PSD length}/2)^2 \times \text{PSD thickness} \times \pi$. Three independent experiments were performed, and at least 50 synapses per condition were analysed.

3.8. Immunoblotting

3.8.1. Lysis and Harvesting

Rat hippocampal neuronal cells were washed once with DPBS and after being scrapped on ice with RIPA buffer (50 mM Tris, pH 8.0, 150 mM NaCl, 0.1% SDS, 0.5% Na-DOC, 100 mM Na-Orthovanadate, 1% NP40 and 1 pill of Proteinase Inhibitor), were subjected to 5 cycles of 10 seconds of sonication. To measure the protein concentration, a Bradford protein assay was performed. Therefore, Bradford solution (160 mg Serva Blue, 85% Phosphoric acid, Ethanol, ddH_2O) was added to a series of BSA standard as well as to protein extract diluted in 15 mM NaCl (both prepared in duplicate). The standards and the samples absorbance were measured at 595 nm with a Spectrophotometer (Labsystems Multiskan RC) and a standard curve was draw in Excel program (Microsoft) to calculate samples concentration.

3.8.2. Protein Electrophoresis and Blotting

After protein quantification, 10 µg of protein extracts were denaturated in 4x loading buffer (200 mM Tris HCl, pH 6.8, 200 mM DTT, 4% SDS, 4mM EDTA, 40% Glycerol, 0.02% Bromophenolblue) and boiled for 3 min at 99ºC. Samples were then loaded alongside with a pre-stained protein marker (PageRuler, Thermo Scientific) in 8% or 12% polyacrylamide gels. The gel chamber was filled with running buffer (25 mM Tris, 250 mM glycine, 0.1% SDS, pH 8.3) and electrophoresis was carried out at 120 V. Protein's separation was followed by blotting at 1.3 A and 28 V for 7 min, onto a nitrocellulose membrane (Bio-Rad), in a Trans-Blot Turbo transfer system (Bio-Rad).

3.8.3. Immunodetection and Quantitative Analysis

The membranes were blocked with 5% Bovine Serum Albumin - Fraction V (BSA, pH 7.0, Bio Froxx) in TBS-T (50 mM Tris-Cl, pH 7.5, 150 mM NaCl, 0.1% Tween 20) for 1h at RT and incubated overnight with the primary antibodies diluted in 5% BSA and TBS-T at 4ºC. After wash 3 times with TBS-T for 30 min, the membranes were incubated with the secondary antibodies in TBS (50 mM Tris-Cl, pH 7.5, 150 mM NaCl) for 1h at RT. Following washing step with TBS-T for a period of 30 min, each protein signals were detected through enhanced chemifluorescence method using ECL (Enhanced Chemiluminescence Substrate, ThermoFisher) and acquired on a MicroChemi 4.2 (Biostep). The protein levels of interest were calculated relative to β-actin levels using ImageJ. Three independent experiments were performed.

3.9. Statistical Analyses

Statistical analyses were performed using Prism (GraphPad Software). Data of three independent experiments are presented as relative to control, as mean ± S.E.M. To determine the statistical significance, data sets were analysed using Two-tailed Mann Whitney test, two-tailed t-test, Two-way ANOVA with Tukey's post-hoc test, One-way ANOVA with Tukey's post-hoc test. P values of <0.05 were considered as significant: *p<0.05, **p<0.01, ***p<0.001, ****p< 0.0001.

4. Results

4. Results

To address the first part of our project, we induced autophagy in primary rat hippocampal neurons (DIV14) through nutrient starvation. This approach (105) inhibits the mTOR activity leading to a reduction of protein synthesis and in parallel upregulates autophagic activity (106). Firstly, we confirmed the induction of autophagy in starved neurons. Neurons that were incubated for 5h with HBSS showed an increased number of somatic p62 (sequestosome-1) puncta (Fig. 3A-B) when compared to untreated cells. p62 is an autophagic receptor, which links ubiquitinated cargos to the inner membrane of the autophagosomes through the interaction with microtubule-associated protein 1 light chain 3 (LC3) (107). To further confirm autophagy induction, we performed immunoblot analysis. Our experiments showed a reduction of total p62 protein level in starved neurons (Fig. 3C-D), indicating an increased autophagic flux in treated cells. When autophagy is induced, in fact, p62 is recruited to the autophagosomes (in line with the increased number of p62-positive structure identified in our immunostaining) and then degraded by the fusion of these structures with the lysosomes (108).
Moreover, we additionally analysed the total LC3-II protein level (the lipidated form of LC3). The conversion of cytosolic LC3-I to membrane bound LC3-II has been associated to autophagosomes formation (107). However, no changes in the LC3-II protein levels were detected between both conditions (Fig. 3E). Nevertheless, LC3-II accumulation might be observable in earlier stages of the treatment since similarly to p62, it is degraded during autophagosome-lysosome fusion (109).

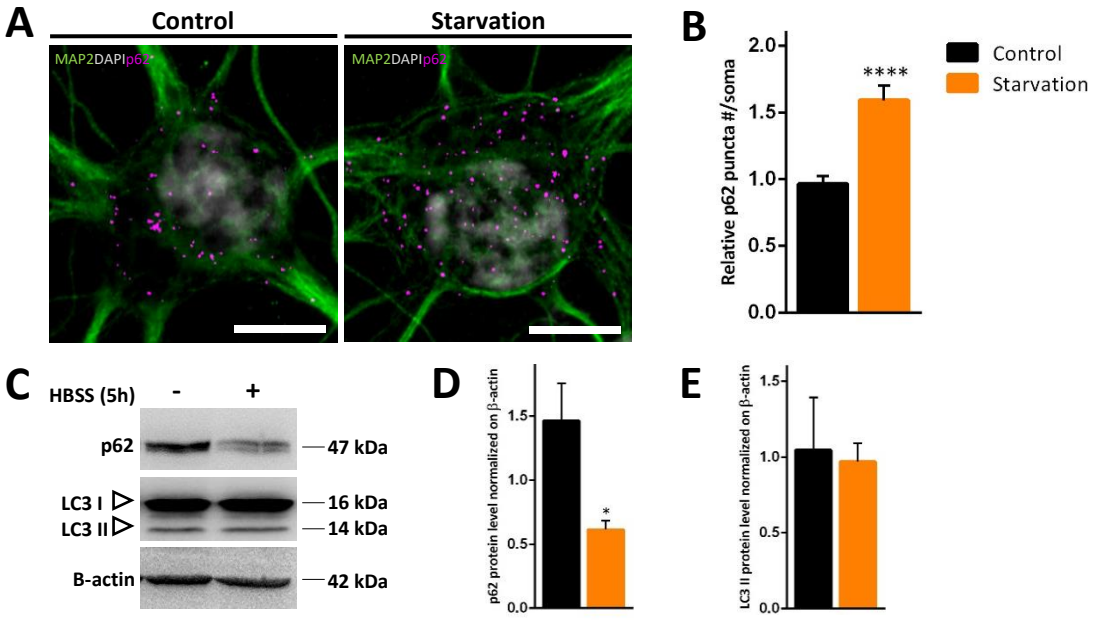

Figure 3 | Neuronal starvation increases the autophagic flux. A, Representative images of primary rat hippocampal neuronal cell soma (DIV14) immunostained against p62. **B**, Analysis of somatic p62 puncta revealed a significant increase in number after starvation ($p<0.0001$). Number of p62 puncta is given as relative to control per soma. For each condition 25–30 neurons from 3 replicate experiments were considered. **C**, Immunoblot showing p62 and LC3 II protein levels, which are quantified in (**D-E**). **D**, p62 protein level was significantly decreased under starvation ($p=0.0474$). **E**, The total LC3-II protein level was not significantly altered by starvation ($p=0.8444$). Data are mean ± S.E.M. Two-tailed Mann Whitney test (**A**) and two-tailed t-test (**D-E**). *$p<0.05$, ***$p<0.001$. Scale bars represent 10 µm.

Together, these observations indicate that 5h of starvation activates the autophagic pathway in neuronal cells, enabling us to investigate the possible contribution of autophagy in synaptic remodelling.

The first question that we were addressing was the impact of autophagy on the morphology of synapses. To that end, we performed TEM to visualize and analyse the synaptic ultrastructure. Interestingly, we observed a significant reduction of the PSD volume in starved neurons in comparison to untreated cells (Fig. 4A-B), demonstrating that autophagy activation leads to PSD composition changes. Since the PSD is mainly constituted by scaffold proteins, which play a crucial role in synapse integrity (31), we further analysed the synaptic cleft width. Starved neurons showed increased width of the synaptic cleft (Fig. 4C), suggesting that the loss of PSD elements might affect the synaptic integrity by disrupting the structural contacts between the pre- and post-synapse. This findings led to the hypothesis that nutrient starvation could also affect synaptic transmission. This hypothesis was indeed strengthened by a reduced number of pre-synaptic vesicles (PSVs) in HBSS-treated neurons (Fig. 4D). However, no significant changes were observed in docked PSVs number between starved neurons and control (Fig. 4E).

Since our ultrastructural studies revealed that autophagy induction leads to dramatic morphological changes at synapses, we next investigated how pre- and postsynaptic molecules are affected.

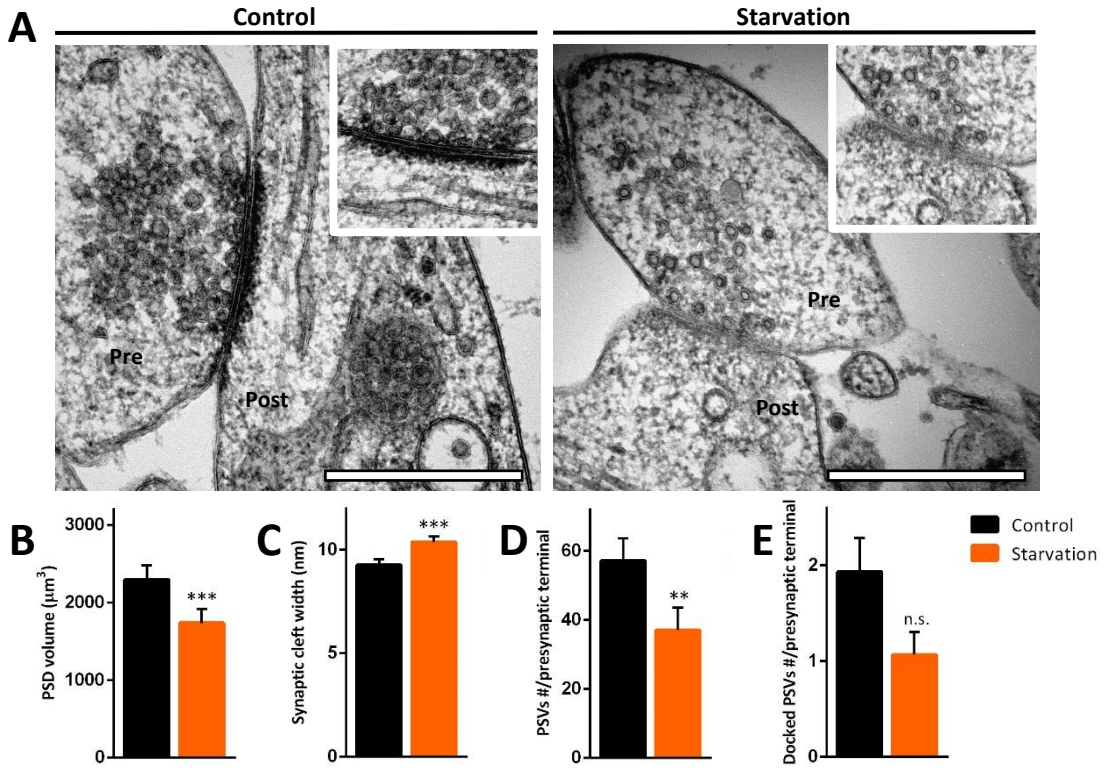

Figure 4 | Synapses undergo ultrastructural changes in starved neurons. A, Representative transmission electron microscopy images of primary rat hippocampal neuronal synapses (DIV14) stained with lead citrate (Pre - presynaptic terminal; Post – postsynaptic terminal). **B**, After starvation treatment, PSD thickness was reduced in comparison to non-treated neurons (p=0.0006). **C**, The synaptic cleft width was increased in starved neurons (p=0.0001). **D-E**, Quantification of PSVs structures. Presynaptic terminals of starved neurons contain significantly less PSVs structures (p=0.0072). (**D**), but show no significant differences in docked PSVs structures number (p=0.0735) (**E**). Images were acquired from 3 independent specimens, and 45–50 synapses in each condition were evaluated. Data are mean ± S.E.M. Two-tailed Mann Whitney test. **p<0.01, ***p<0.001. Scale bars represent 500 nm.

Given the crucial role of Shank scaffold proteins in the molecular organization of the PSD (5-7), we evaluated the Shank2- and Shank3 clusters number and size along the dendrites after starvation. In line with our ultrastructural findings, starved neurons showed a significant down-regulation of Shank2 clusters number and size (Fig. 5A-C) in comparison to control. In contrast, starvation had no significant impact on Shank3, as no changes in clusters number and size were detected (Fig. 5D-F). These findings, suggest that starvation-induced autophagy selectively affects the PSD composition.

Based on these results, we further analysed the impact of HBSS treatment on Homer, a well-known Shank-interacting protein (9). No significant effects were observed in Homer clusters number after starvation (Fig. 5G-H). However, starved neurons showed reduced size of Homer clusters in comparison to untreated cells (Fig. 5I), corroborating the idea that autophagy contributes in synaptic remodelling.

Recent studies have shown that the Bassoon protein of the presynaptic active zone maintain the synapse viability by regulating local protein ubiquitination (110) and autophagy (103). These processes are stimulated by the E3 ubiquitin ligase Siah1 and autophagy-related protein 5 (ATG5) respectively, whose functions are negatively regulated via binding to Bassoon. Therefore, we next investigated how this presynaptic scaffold protein reacts in response to autophagy induction. Interestingly, Bassoon clusters number and size dramatically decreased after starvation (Fig. 5J-L). This observation, strongly suggests that Bassoon undergoes a fast downregulation during cell starvation, which might enable the presynaptic remodelling by local protein ubiquitination and autophagy.

Since our findings in starved neurons show a dramatic PSVs number reduction, synaptic cleft width increased and Bassoon down-regulation, we next focused our analysis on NMDARs, which are regulated in an activity-dependent manner (111). We observed no significant differences in NR1-positive clusters number (Fig. 5M-N) between both conditions. However, the NR1-positive clusters were found bigger in starved neurons in comparison to control (Fig. 5O). These results indicate that starvation-induced autophagy might lead to NMDARs internalization into recycling vesicles (111), where they form larger clusters. Moreover, they also suggest a possible deregulation of synaptic activity induced by cell starvation.

In order to understand whether these mechanisms are restricted to excitatory synapses, we further analysed the Gephyrin-positive clusters, a well-known postsynaptic scaffold protein of inhibitory synapses (112-113). Starved neurons showed no changes in Gephyrin clusters number (Fig. 5P-Q), but a decreased in their size in comparison to untreated neurons (Fig. 5R).

Altogether, our findings confirmed the idea that synapses undergo structural and molecular remodelling in response to autophagy. Moreover, in accordance to our data, PSD structural changes occur in parallel with a Shank2 down-regulation suggesting that Shank proteins are involved in this remodelling process.

Given these interesting evidences we next investigate the specific contribution of Shanks in neuronal morphology and at synaptic micro-environment. To this aim we generated a new double *Shank2 Shank3* conditional KO mouse line – *Shank2*$^{flx/flx}$ *Shank3*$^{flx/flx}$ – in which the SHANK2 PDZ domain and the SHANK3 SH3 domain are flanked by two loxP sites (floxed) of the same direction (Fig. 6A-B) – see **2. Aim** and Schmeisser *et al*., (88).

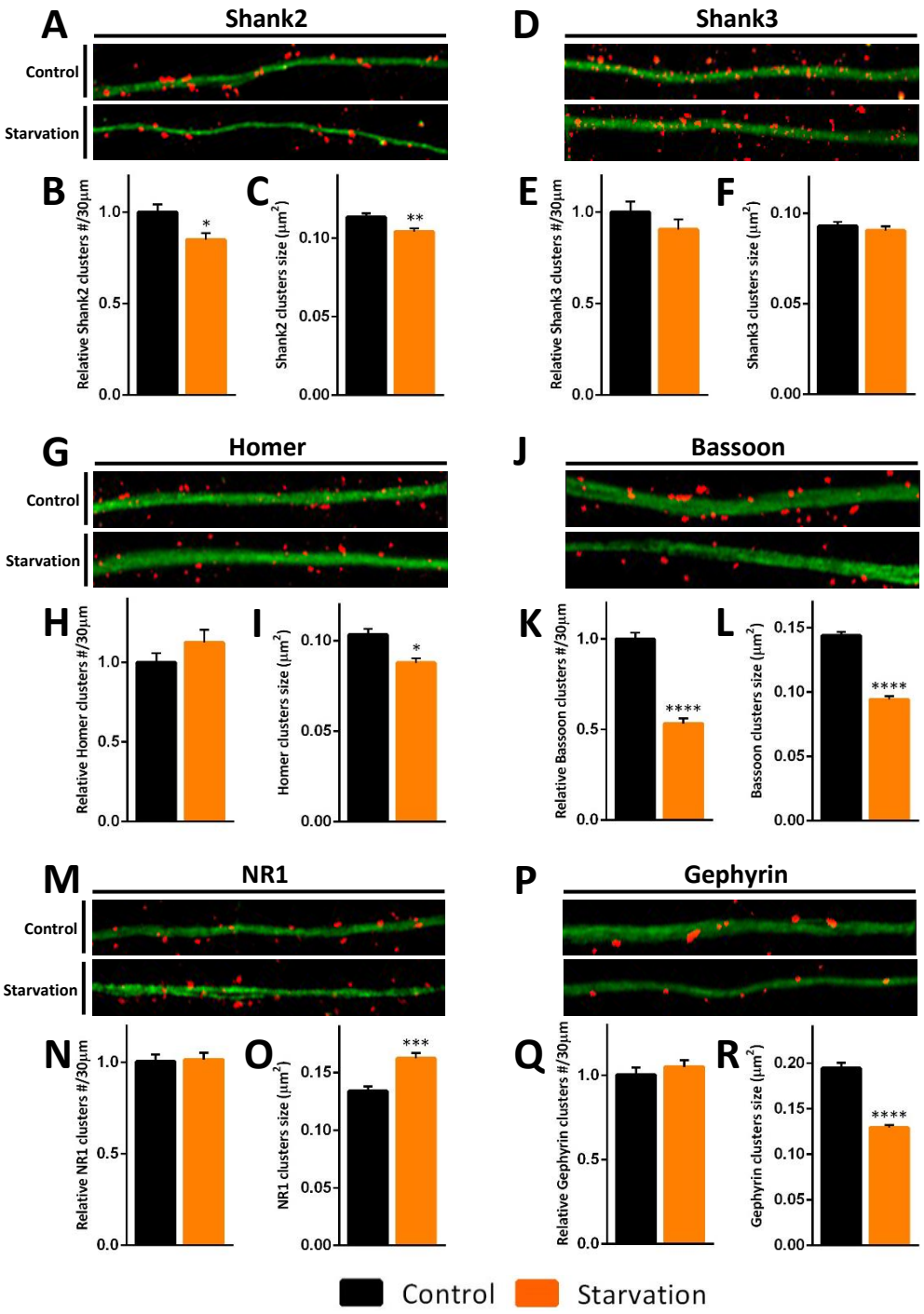

Figure 5 | Starvation-induced autophagy affects synaptic molecular composition. A, **D**, **G**, **J**, **M** and **P**, Representative images of dendrites (30 µm) of control and starved primary rat hippocampal neurons (DIV14) immunostained against MAP2 (green) and Shank2 (**A**); Shank3 (**D**); Homer (**G**); Bassoon (**J**); NR1 (**M**) and Gephyrin (**P**) (red). **B**-**C**, Quantification of Shank2 clusters revealed a significant decrease in average number (p=0.0315) (**B**) and size (p=0.0016) (**C**) within 5h of starvation. **E**-**F**, Starvation treatment exerts no significant effects in Shank3 clusters number (p=0.0502) (**E**) and size (p=0.4979) (**F**), as shown by quantification. **H-I**, Analysis of Homer clusters revealed no significant changes in number (p=0.7304) (**H**), but a decreased in size (p=0.0293) (**I**) after starvation. **K**-**L**, Quantification revealed that Bassoon clusters number (p<0.0001) (**K**) and size (p<0.0001) (**L**) significantly decrease under starvation. **N**-**O**, In starved neurons, no significant changes were detected in NR1 clusters number (p=0.7165) (**N**), while their size were increased (p=0.0006) (**O**), as revealed by quantification. **Q**-**R**, Analysis of Gephyrin clusters revealed no significant changes in their number (p=0.1677) (**Q**), but a reduction in size (p<0.0001) (**R**). Number of clusters are given as relative to control per 30 µm. For each condition 25–30 neurons from 3 independent experiments were analysed. Data are mean ± S.E.M. Two-tailed Mann Whitney test. *p<0.05, **p<0.01, ***p<0.001, ****p< 0.0001.

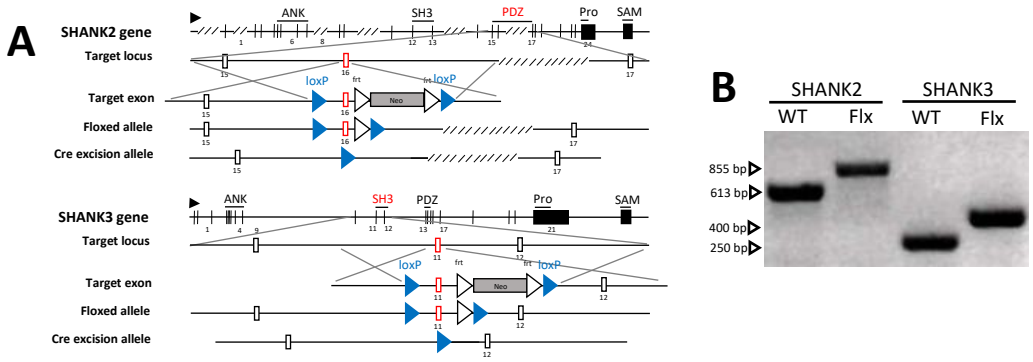

Figure 6 | Generation of *Shank2*$^{flx/flx}$ *Shank3*$^{flx/flx}$ mouse line. A, Schematic targeting strategy for *Shank2*$^{flx/flx}$ *Shank3*$^{flx/flx}$ mouse line. **B**, PCR products amplified showing the bands of *Shank2* WT, *Shank2*$^{flx/flx}$, *Shank3* WT and *Shank3*$^{flx/flx}$ genes for animal genotyping.

As we are interested in study the potential effects induced by Shank2 and Shank3 loss during neuronal development of distinct cell populations we established primary mouse hippocampal and cortical neuronal cell cultures isolated from *Shank2*$^{flx/flx}$ *Shank3*$^{flx/flx}$ embryonic mice (Fig. 7A). Based on the Cre-loxP recombination principles (114), floxed sequences can be excised in the presence of Cre-recombinase, which enables the temporal control of expression of the targeted genes. Thus, to disrupt SHANK2 and SHANK3 genes in our model, different Cre-recombinase delivery strategies, such us viral transduction and TAT peptide-mediated cellular delivery (Fig. 7B) were tested. Co-labeling experiments against MAP2 and GFP (to increase the intrinsic Cre-GFP signal at nucleus) revealed that AAV9-Syn-Cre-GFP virus successfully transduced neurons (Fig. 7B, e).

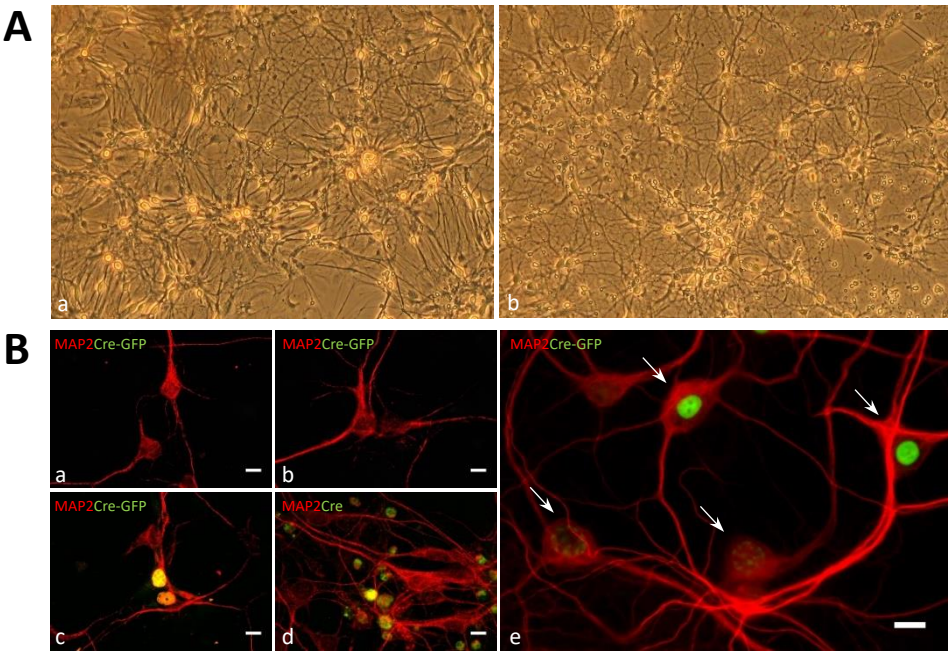

Figure 7 | Establishment of primary mouse hippocampal and cortical neuronal cell cultures derived from *Shank2*$^{flx/flx}$ *Shank3*$^{flx/flx}$ embryonic mice. **A**, Representative phase contrast microscopy images of primary mouse hippocampal (**a**) and cortical (**b**) neurons at DIV14. **B**, **a-c** and **e**, Representative images of primary mouse hippocampal neurons infected at DIV7 with AAV2-CMV-Cre-GFP (MOI 100.000) (**a**), AAV5-CMV-Cre-GFP (MOI 100.000) (**b**), CMV-Cre-GFP-Lentivirus (MOI 2.5) (**c**), AAV9-Syn-Cre-GFP (MOI 100.000) (**e**) and immunostained against MAP2 and GFP at DIV14. **B**, **d**, Representative images of primary mouse hippocampal neurons (DIV7) treated with TAT-Cre Recombinase (0.75 µM) for 6h and immunostained against MAP2 and Cre-recombinase (Cre). Arrows indicate neurons positive for both MAP2 and GFP. Scale bars represent 10µm.

To answer our questions we transduced primary mouse hippocampal and cortical neuronal cells at different stages of development (DIV3, DIV7 and DIV14) and analyzed them at DIV20.
Initially, we confirmed whether the transduction of both cell cultures leads to Shank2 and Shank3 proteins deficiency. At DIV20, primary hippocampal and cortical GFP-positive neurons showed remarkable reduction of Shank2- and Shank3 positive-clusters number (Fig. 8A-F), indicating that viral transduction with AAV9-Syn-Cre-GFP lead to the loss of both Shank proteins. Moreover, this result was observed independently from the time of cell transduction allowing us to investigate whether there is a critical time window in which Shank2 and Shank3 are crucial for the neuronal development.

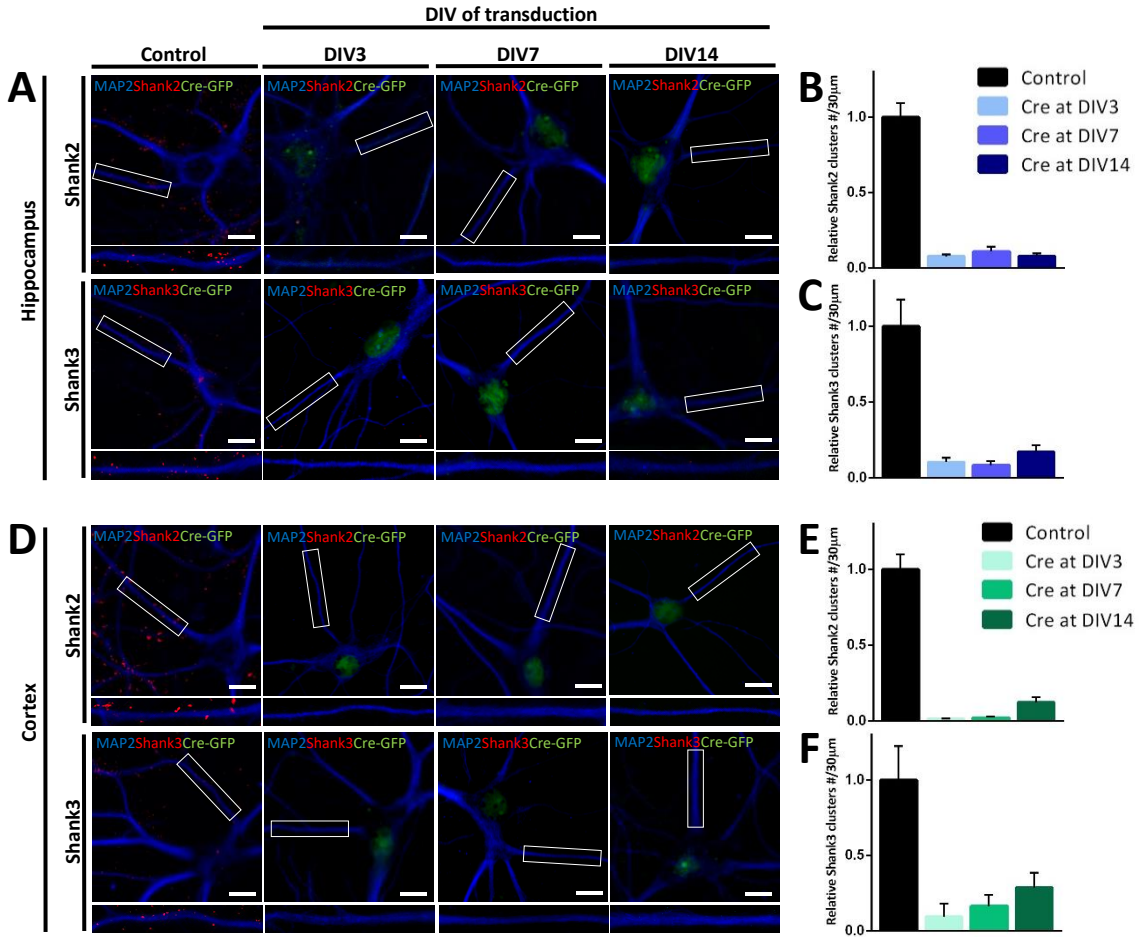

Figure 8 | Primary mouse hippocampal and cortical neuronal cells transduced with AAV9-Syn-Cre-GFP show Shank2 and Shank3 proteins loss. A and **D**, Representative images of primary mouse hippocampal neurons (Hippocampus) (**A**) and primary mouse cortical neurons (Cortex) (**B**) at DIV20 not treated (Control) or transduced with AAV9-Syn-Cre-GFP (MOI 100.000) at DIV3; DIV7; or DIV14. Representative images of dendrites (30 µm) are shown below. Neuronal cells were immunostained against Shank2 or Shank3. **B-C** and **E-F**, Transduction of primary mouse hippocampal (**B-C**) and cortical (**E-F**) neurons results in a strong reduction of Shank2 (**B** and **E**) and Shank3 (**C** and **F**) clusters number. Number of clusters are given as relative to control per 30 µm. For each condition a minimum of 10 neurons from 1 experiment were analysed. Scale bars represent 10µm.

Shank2 and Shank3 are considered master scaffolding proteins at excitatory synapses (14). One question that we were interested to answer was if the loss of these synaptic proteins could influence neuronal morphology. Therefore, we traced dendrites of primary hippocampal and cortical neurons (DIV20) through MAP2 staining to investigate their arborisation complexity. Sholl analysis revealed that the dendritic arborisation of primary hippocampal neurons

transduced at DIV3 and DIV14 was reduced, while the transduction of the same neurons population at DIV7 led to an increase of dendritic complexity (Fig. 9A). These observations suggest that the loss of Shank2 and Shank3 leads to distinct abnormal neuronal morphology depending on the specific stage of development in which they were disrupted. In contrast, the loss of these two major synaptic proteins exerts no significant effects in primary cortical neurons morphology (Fig. 9B), indicating that hippocampal neuronal population might be more sensible to Shank2 and Shank3 deficiency. To test this hypothesis we next focus our studies at synaptic micro-environment where the loss of Shank2 and Shank3 proteins could be more pronounced.

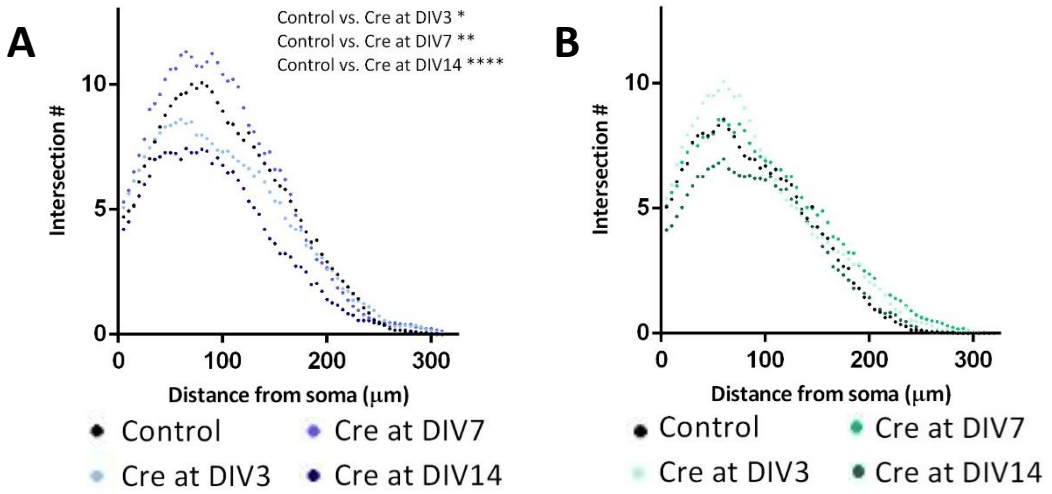

Figure 9 | Shank2 and Shank3 loss affects neuronal complexity. A, Sholl analysis revealed a decrease of neuronal complexity of primary mouse hippocampal neurons transduced at DIV3 (Cre at DIV3) and at DIV14 (Cre at DIV14) and an increase of neuronal complexity when transduced at DIV7 (Cre at DIV7). **B**, No significant effects were observed in transduced primary mouse cortical neurons in comparison to control cells. For each condition 10 neurons from 3 independent experiments were analysed. Data are mean. Mean ± S.E.M are shown in Supplementary Fig. 1. Two-way ANOVA with Tukey's post-hoc test. *p<0.05, **p<0.01, ****p< 0.0001.

As have been reported in this work, Shank family members form large platforms at PSD together with Homer protein (8). To determine whether this Shank-binding partner is affected by the loss of Shank2 and Shank, we analysed Homer-positive clusters along the dendrites of primary hippocampal and cortical neurons at DIV20. In comparison to control cells, transduced primary hippocampal and cortical neurons showed a strong reduction in Homer clusters number (Fig. 10A-C). In line with the previous Sholl analysis, these changes might be more dramatic in hippocampal than in cortical neuronal population. Nevertheless, this effect was observed independently from the stage of neuronal development in which Shank2 and Shank3 protein expression was compromised. Taken together, all these observations support the idea that Shank proteins are crucial for the proper PSD assembly as well as dendritogenesis.

Additionally, we analysed the Bassoon-positive clusters to clarify whether Shank2 and Shank3 deficiency also affects the presynaptic terminals. Surprisingly, the loss of both Shanks at early stages of development (DIV3) leads to a remarkable increase of Bassoon clusters number in primary hippocampal cells (Fig. 10D-E). This could suggest that neurons undergo a compensatory mechanism to overcome the possible postsynaptic impairment. However, no significant changes in Bassoon clusters number were observed in primary cortical cells transduced at DIV3 (Fig. 10D, F). On the other hand, we found a strong downregulation of Bassoon clusters number in both neuronal populations transduced at DIV7 or at DIV14 (Fig. 10D-F). As mentioned above - see **1.2. Shank proteins in neuronal development** - excitatory synapses are found built only after DIV7

and become more complex over time (47). Therefore, the Shank2 and Shank3 loss at later stages (from DIV7 on) might lead to the disruption of those synaptic contacts and consequently, to a down-regulation of Bassoon.

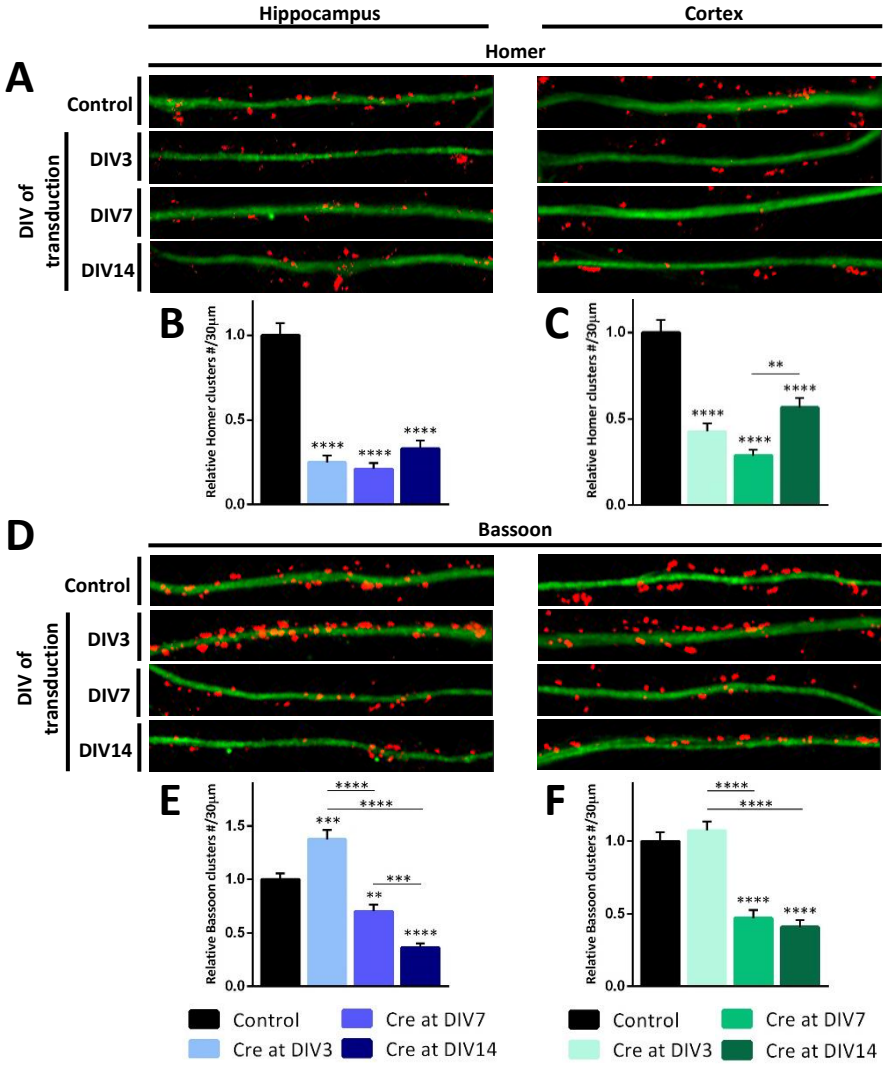

Figure 10 | Shank2 and Shank3 proteins loss affects pre- and postsynaptic markers of primary mouse hippocampal and cortical neurons. A and **D**, Representative images of dendrites (30 µm) of primary mouse hippocampal neurons (Hippocampus) and primary mouse hippocampal neurons (Cortex) at DIV20 not treated (Control) or transduced with AAV9-Syn-Cre-GFP (MOI 100.000) at DIV3; DIV7; or DIV14. Neuronal cells were immunostained against MAP2 (green) and Homer (red) (**A**) or MAP2 (green) and Bassoon (red) (**D**). **B** and **C**, Quantification of Homer clusters number along dendrites of primary mouse hippocampal (**B**) and cortical (**C**) neurons. Neuronal transduced cells show a significant reduction in Homer clusters number when compared to control cells. **E** and **F**, Quantification of Bassoon clusters number along dendrites of primary mouse hippocampal (**E**) and cortical (**F**) neurons. Primary hippocampal neurons show a significant increase of Bassoon clusters number when transduced at DIV3 but a Bassoon clusters number reduction when transduced at DIV7 and DIV14 (**E**). No significant changes in Bassoon clusters number were found between primary cortical neuronal cells transduced at DIV3 and control, while a significant reduction of Bassoon clusters number were observed in primary cortical neuronal cells transduced at DIV7 and DIV14 (**F**). Number of clusters are given as relative to control per 30 µm. For each condition a minimum of 10 neurons from 3 independent experiments were analysed. Data are mean ± S.E.M. One-way ANOVA with Tukey's post-hoc test. **p<0.01, ***p<0.001, ****p< 0.0001.

Since our initial findings revealed that autophagy induction results in a dramatic Bassoon cluster number reduction, we evaluated the autophagic flux after Shank2 and Shank3 loss. Both hippocampal (Fig. 11A-B) and cortical (Fig. 11C-D) populations showed similar somatic p62

puncta number in comparison to control cells. Only a minor reduction of p62 puncta number was observed in primary hippocampal neurons transduced at DIV14 (Fig.11A-B). Taken together, these observations suggest that Shank2 and Shank3 deficiency exert no relevant effects on autophagy. Nevertheless, autophagy is a highly dynamic mechanism, which can be modulated overtime in response to intra- and extracellular stimulus (107). Thus, the loss of both Shank proteins could induce changes in autophagic flux at earlier or later stages of development.

In order to have a more complete idea of Shank2 and Shank3 loss impact at synaptic micro-environment we further started to analyse other synaptic elements, including NR1 and Gephyrin. Similarly to our previous analysis, we evaluated the positive-clusters of those markers along the dendrites of control cells and transduced primary hippocampal and cortical neurons at DIV3, DIV7 and DIV14. To date we have performed 2 independent experiments. Although we are not able to define conclusions, these preliminary data suggest that there is a tendency of a reduction of NR1-positive puncta number in both neuronal populations transduced (Supplementary Fig. 2A-B). Moreover, the loss of Shank2 and Shank3 seem to exert no dramatic changes on Gephyrin-positive puncta number (Supplementary Fig. 2C-D).

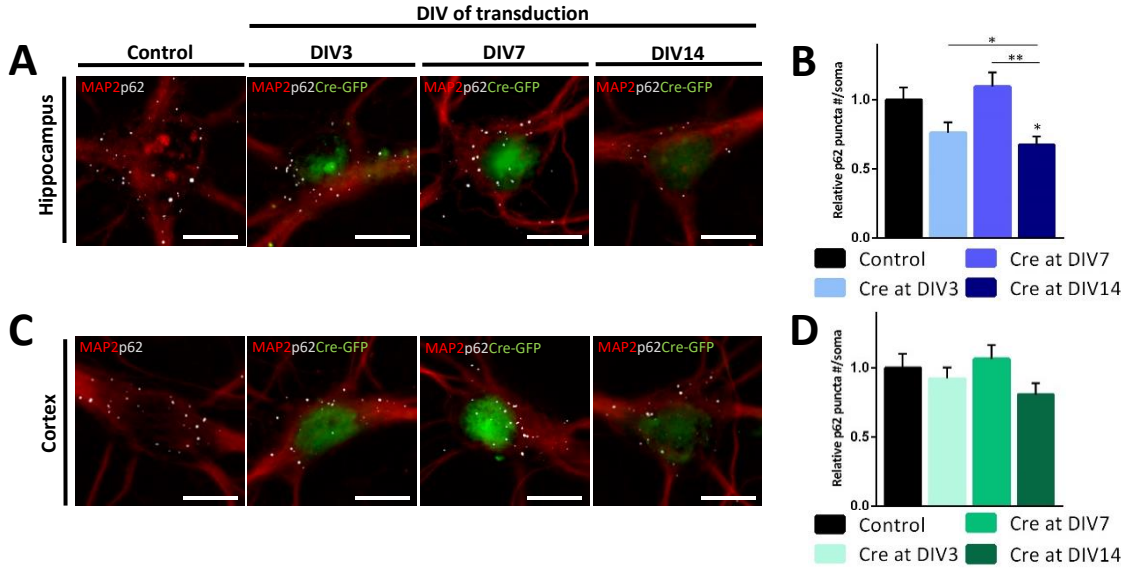

Figure 11 | Autophagic flux in Shank2 and Shank3 deficient primary mouse hippocampal and cortical neurons. A and **C**, Representative images of primary mouse hippocampal (**A**) and cortical (**C**) neuronal cell soma (DIV20) not treated (Control) or transduced with AAV9-Syn-Cre-GFP (MOI 100.000) at DIV3; DIV7; or DIV14. Neuronal cells were immunostained against p62. **B**, No significant changes were observed in primary mouse hippocampal neuronal cells transduced at DIV3 and DIV7, while the same cells transduced at DIV14 showed a slightly decrease in p62 puncta number in comparison to control. **D**, Analysis of somatic p62 puncta revealed no significant changes in its number between transduced primary mouse cortical neurons and control cells. Number of p62 puncta is given as relative to control per soma. For each condition a minimum of 19 neurons from 3 independent experiments were analysed. Data are mean ± S.E.M. One-way ANOVA with Tukey's post-hoc test. *p<0.05. Scale bars represent 10µm.

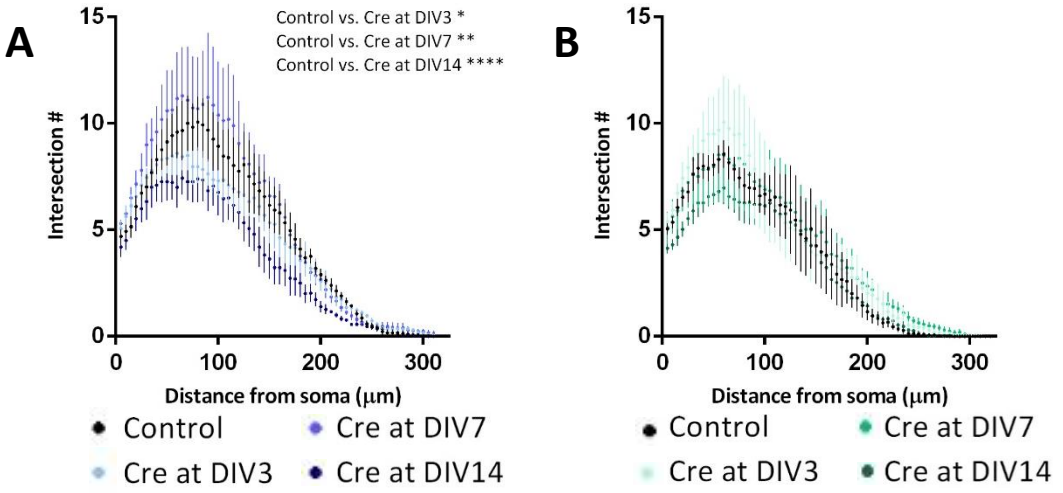

Supplementary Figure 1 | Shank2 and Shank3 loss affects neuronal complexity. Supplementary figure related to Figure X showing data as mean ± S.E.M. Two-way ANOVA with Tukey's post-hoc test. *p<0.05, **p<0.01, ****p< 0.0001.

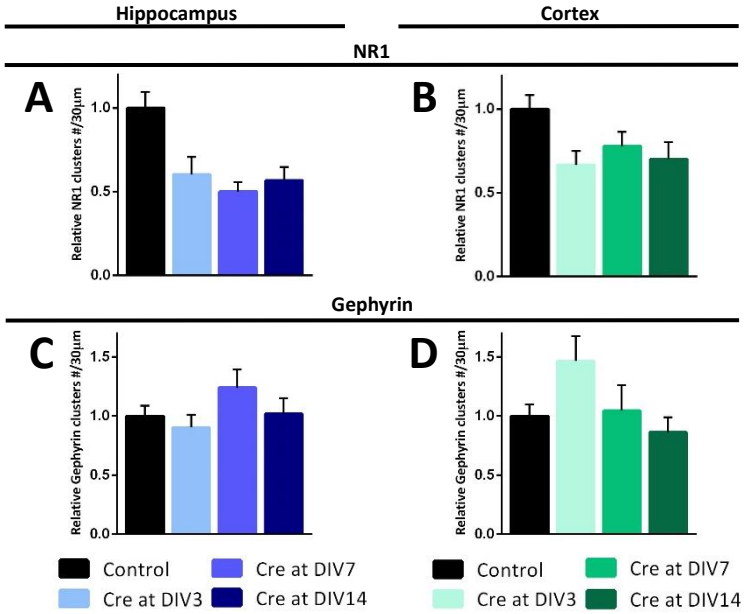

Supplementary Figure 2 | NR1- and Gephyrin clusters number analysis in Shank2 and Shank3 deficient primary mouse hippocampal and cortical neurons. A-B, Analysis of NR1 clusters number along dendrites of primary mouse hippocampal (**A**) and cortical (**B**) neurons. **C-D**, Analysis of Gephyrin clusters number along dendrites of primary mouse hippocampal (**C**) and cortical (**D**) neurons. Number of clusters are given as relative to control per 30 μm. For each condition a minimum of 10 neurons from 2 independent experiments were analysed.

5. Discussion

5. Discussion

Shank scaffolding proteins are located at PSD of excitatory synapses, where they act as intracellular anchors to support synaptic integrity and provide the dynamics required for synaptic remodelling (6, 8, 10). By altering specific cues, such as synaptic strength, synapses can modulate their molecular composition and morphology in order to adjust their function to the environmental conditions (54).

Using an *in vitro* system (primary neuronal culture) we induced synaptic structural and molecular changes through starvation-induced autophagy to better elucidate Shanks contribution in synaptic remodelling. Under these conditions we observed a selective down-regulation of Shank2, while Shank3 was not significantly affected. This suggests that Shank2 might be more prone to undergo dynamic changes in comparison to Shank3, which seems to be stabilized at synapses. In fact, previous studies have been indicating that different Shank proteins play distinct roles at synapses and might also be involved in distinct signalling pathways (39, 49).

Since we were interested in investigating not only the molecular changes occurring in response to nutrient starvation, but also the possible structural modifications induced at the synapses when mTOR is inhibited, we performed TEM analysis after High pressure freezing fixation. The extremely high quality of the samples achieved with this particular technique allowed us to identify, in accordance with Shank2 down-regulation, a dramatic reduction of the PSD volume in starved neurons. Moreover, the same cells presented increased width of the synaptic cleft, strongly suggesting that the loss of PSD elements compromise the synaptic integrity. The physical linkage between pre- and post-synapse, which is supported by cell adhesion molecules and scaffolding proteins is in fact crucial for the maintenance of synaptic transmission (31). In agreement with this, we observed less PSVs at presynaptic terminals of starved neurons indicating that autophagy not only modulates morphological changes but may also affects synaptic activity.

These variations, referred to as synaptic plasticity, are crucial for the maturation of synaptic contacts and for the normal course of circuitry development (43). Moreover, they are thought to underlie fundamental functions of the mammalian brain, such as learning and memory formation (31-32). Playing such an important role in several cognitive activities, impairment in synaptic plasticity can engender critical consequences affecting human cognition and lead also to neuropsychiatric diseases, including Autism Spectrum Disorders (72). Mutations in the SHANK genes, in particular SHANK2 and SHANK3, have been associated to ASDs, which features abnormalities in synaptic structure and function, as well as, circuitry defects (86).

Since these results suggests a specific contribution of Shank2 in synaptic remodelling under synaptic plasticity induction, we then investigated how the absence of the two scaffold proteins in different stages of neurodevelopment could affect the synaptic ultrastructure and composition. To address this, we established primary hippocampal and cortical neuronal cell cultures derived from *Shank2*$^{flx/flx}$ *Shank3*$^{flx/flx}$ mice which could enable us to selectively knock-down these two ASD-related proteins.

Considering that previous studies have linked dendritic arborisation abnormalities to neurotransmission and circuitry defects induced by disruption of SHANK family genes (24, 115) we first investigate how the loss of Shank2 and Shank3 at different stages of development may affect the dendritic complexity. We found that Shank2 and Shank3 loss affects the dendritic

arborisation development of primary mouse hippocampal neuronal cells. Interestingly, these morphological changes were distinct depending on the specific stage of neuronal development in which SHANK2 and SHANK3 genes were disrupted. The loss of Shank2 and Shank3 at earlier stages of development (DIV3) and at mature stages (DIV14) led to a reduction in complexity of dendritic arborisation. However, the opposite effect (neuronal hypertrophy) was observed when SHANK2 and SHANK3 genes were disrupted at DIV7, a cell culture neurodevelopment stage in which the axon is already matured. As these data suggest, Shank scaffolding proteins might be involved in distinct process during neuronal development. Moreover, previous studies have been suggesting that Shank proteins contribute to the development of other neuronal structures in addition to synapses, such as growth cones (1, 42, 48) and presynaptic terminals (48). Giving these considerations, both Shank2 and Shank3 proteins might be involved in mechanisms of neurite arborisation and their loss at different time points may disrupt/interrupt distinct steps of the pathway.

The wide range of autism-associated behaviours observed in ASD cases carrying mutations in SHANK genes family have been partially explained by which SHANK gene or protein isoform is affected. Nevertheless, recent studies have highlighted the possibility that specific brain regions might be more susceptible to SHANK genes disruption and are more likely to contribute to ASD onset (24, 88, 94). Consistent with this, and in contrast with hippocampal analysis, we observed that Shank2 and Shank3 deficiency exerts no effects in the development of dendritic arborisation of primary mouse cortical neurons. Therefore, Shank proteins may contribute to different development pathways in distinct cell types giving a start point for further experiments.

At PSDs, Shank proteins directly bind Homer to stabilize mGluR1 and mGluR5 at postsynaptic membrane (9). Dysregulation of this complex has been identified as a risk factor for ASD (26). Moreover, different studies performed in *Shank*-mutated mouse models have been showing that Homer scaffolding protein is dramatically affected in concomitance with the disruption of SHANK genes (24, 89, 94). In line with this, we observed that Shank2 and Shank3 deficiency results in a strong reduction of Homer-positive clusters number along the dendrites. Interestingly, the magnitude of this phenotype appears to be higher in hippocampal cells in comparison to cortical cells, highlighting the heterogeneous vulnerability of different cell types to Shanks deficiency. Importantly, the down-regulation of this Shank-binding partner was induced independently from the stage of neuronal development in which both Shank proteins were compromised. Together, these evidences indicate that the key role of Shank proteins family as organizers of PSD architecture is always required during synaptogenesis.

In contrast, during autophagy-mediated synaptic remodelling only a minor reduction of Homer clusters size was observed. Since Shank proteins play such important role in organizing intermediate scaffolding proteins at PSD and only a slight down-regulation of Shank2 occurred during neuronal starvation, Homer protein seems to remain stabilized at PSD by Shank proteins even under synaptic remodelling.

In this study, we also provide some evidences that the downregulation of Shank proteins in both model systems may result in a decreased synaptic transmission. For instance, in addition to the reduction of PSVs number at presynaptic specialization, the synaptic molecular changes induced by nutrient starvation might lead to an internalization of NMDA receptors into recycle vesicles as suggested by the increase of NR1 clusters size. Moreover, our preliminary results in the double KO mice suggest that there is a tendency of a reduction of NR1-positive clusters number

along the dendrites of Shank2 and Shank3 deficient primary hippocampal and cortical neurons, corroborating the idea that the loss of Shank proteins might compromise the NMDAR clustering at synapses.

Furthermore, our data suggest that the effects induced by Shank2 and Shank3 deficiency during neuronal development might be specific to excitatory synapses, since no drastic changes have been observed in Gephyrin scaffolding protein analysis. However, when synaptic remodelling is induced by activation of autophagy both excitatory and inhibitory synapses seem to undergo molecular changes as shown by the reduction of Gephyrin clusters size.

Taken together these results obtained in both model suggest that morphological and molecular changes at synapses can lead to impairments in synaptic transmission. Previous studies have described that synaptic transmission can be controlled by the crosstalk between pre- and postsynaptic terminals, as in the case of the endocannabinoids which can mediate the presynaptic neurotransmitter release, as reviewed in (116). Considering this evidence, we investigate the possible contribution of the pre-synapses in the changes previously observed. Interestingly, we found a strong down-regulation of the presynaptic scaffold protein Bassoon in starved neurons. To our knowledge, this molecular alteration indicates for the first time that Bassoon can undergo such fast and dynamic process even besides its large size and tight association with the active zone. Moreover, since Bassoon mediates negatively the autophagic process (103) and we induced synaptic remodelling through activation of autophagy, Bassoon might be removed from synapses to allow the clearance of synaptic proteins.

Moreover, a synaptic crosstalk may also take place during synaptogenesis since the contact between an axonal growth cone and a dendrite triggers a rapid recruitment of pre- and postsynaptic markers in order to coordinate a correct presynaptic and postsynaptic growth (43). Indeed, our results suggest that the potential impairment of PSD assembly induced by Shank2 and Shank3 loss at earlier stages of development (DIV3) may lead to further abnormalities at presynaptic site, as indicated by the strong up-regulation of Bassoon in primary hippocampal cells. Interestingly, the opposite effect (Bassoon down-regulation) was triggered by Shank2 and Shank3 loss at later stages of development (DIV7 and DIV14) in hippocampal neuronal cells. Together, our findings suggest that under abnormal postsynaptic assembly the primary hippocampal neuronal cells might increase the number of presynaptic sites to overcome the synaptogenesis impairment. However, when the loss of Shank2 and Shank3 occur after the synapses are already built (from DIV7 on) the integrity of those synaptic contacts might be compromised leading to a down-regulation of Bassoon, as well as, Homer scaffolding proteins.

In contrast with primary hippocampal neuronal cells, the loss of Shank2 and Shank3 at DIV3 in primary cortical neuronal cells seems to exert no significant effects in Bassoon clusters number. One possible explanation for this, is that the assembly of cortical synaptic contacts might undergo different mechanisms, such as recruitment of other postsynaptic scaffolding proteins to compensate the absence of Shank2 and Shank3 proteins. Nevertheless, once the synaptic contacts are established (from DIV7 on), the loss of Shank2 and Shank3 seems to induce similar abnormalities independently to cell type, as revealed by the strong down-regulation of Bassoon. Since autophagic defects have been linked to synaptic impairments in some ASD clinical cases (70), the down-regulation of Bassoon protein observed in both neuronal populations which lost Shank2 and Shank3 at DIV7 and DIV14 could suggest that the autophagic flux would be increased. Although no relevant changes were observed, it is well-described that this degradative mechanism can be modulated in response to a wide range of intra- and extracellular

stimulus overtime (107). Therefore, potential changes in autophagic pathway might be triggered at different stages of synaptogenesis.

In summary, we provided evidences that two ASD-related proteins, Shank2 and Shank3, might be involved in different cell signalling pathways during synaptic remodelling probably to provide distinct structural and molecular dynamics. Moreover, we also demonstrated that the loss of Shank2 and Shank3 strongly affects postsynaptic assembly during the whole synaptogenesis process and as a consequence, further abnormalities at presynaptic level are triggered. Interestingly, these abnormalities seem to be variable depending to the stage of neuronal development in which Shank2 and Shank3 were compromised suggesting that Shank proteins may play distinct roles during certain stages of synaptogenesis. Finally, the potential synaptic impairment underling Shank2 and Shank3 loss seems to affect differentially the neuronal development of primary hippocampal and cortical neurons highlighting the idea that different cellular populations are more vulnerable to Shank proteins deficiency.

6. References

6. References

1. Du, Y., Weed, S.A., Xiong, W.C., Marshall, T.D. and Parsons, J.T. (1998). Identification of a novel cortactin SH3 domain binding protein and its localization to growth cones of cultured neurons. Molecular and Cellular Biology. 18, 5838-51
2. Naisbitt, S., Kim, E., Tu, J.C., Xiao, B., Sala, C., Valtschanoff, J., et al. (1999). Shank, a novel family of postsynaptic density proteins that binds to the NMDA receptor/PSD-95/GKAP complex and cortactin. Neuron. 23, 569-82
3. Böckers, T.M., Kreutz, M.R., Winter, C., Zuschratter, W., Smalla, K.H., Sanmarti-Vila, L., et al. (1999). Proline-rich synapse-associated protein-1/cortactin binding protein 1 (ProSAP1/CortBP1) is a PDZ-domain protein highly enriched in the postsynaptic density. The Journal of Neuroscience. 19, 6506-18
4. Lim, S., Naisbitt, S., Yoon, J., Hwang, J.I., Suh, P.G., Sheng, M. and Kim, E. (1999). Characterization of the Shank family of synaptic proteins. Multiple genes, alternative splicing, and differential expression in brain and development. The Journal of Biological Chemistry. 274, 29510-8
5. Sheng, M. and Kim, E. (2000). The Shank family of scaffold proteins. Journal of Cell Science. 113, 1851-6
6. Böckers, T. M., Bockmann, J., Kreutz, M. R. and Gundelfinger, E. D. (2002). ProSAP/Shank proteins: a family of higher order organizing molecules of the postsynaptic density with an emerging role in human neurological disease. Journal of Neurochemistry. 81, 903-10
7. Kreienkamp, H. J. (2008). Scaffolding proteins at the postsynaptic density: Shank as the architectural framework. Handbook of Experimental Pharmacology. 365-80
8. Sala, C., Vicidomini, C., Bigi, I., Mossa, A. and Verpelli, C. (2015). Shank synaptic scaffold proteins: keys to understanding the pathogenesis of autism and other synaptic disorders. Journal of Neurochemistry. 135, 849–858
9. Tu, J.C., Xiao, B., Naisbitt, S., Tu, J.C., Xiao, B., Naisbitt, S., et al. (1999). Coupling of mGluR/Homer and PSD-95 complexes by the Shank family of postsynaptic density proteins. Neuron. 23, 583–592
10. Sala, C., Piech, V., Wilson, N.R., Passafaro, M., Liu, G.S. and Sheng, M. (2001). Regulation of dendritic spine morphology and synaptic function by Shank and Homer. Neuron. 31, 115–130
11. Gerrow, K., Romorini, S., Nabi, S.M., Colicos, M.A., Sala, C. and El-Husseini, A. (2006). A preformed complex of postsynaptic proteins is involved in excitatory synapse development. Neuron. 49, 547–562
12. Verpelli, C., Dvoretskova, E., Vicidomini, C., Rossi, F., Chiappalone, M., Schoen, M., et al. (2011). Importance of shank3 in regulating metabotropic glutamate receptor 5 (mGluR5) expression and signaling at synapses. Journal of Neurochemistry. 286, 34839–34850
13. Böckers, T.M., Segger-Junius, M., Iglauer, P., Bockmann, J., Gundelfinger E.D. and Kreutz, M.R. (2004). Differential expression and dendritic transcript localization of Shank family members: identification of a dendritic targeting element in the 3'untranslated region of Shank1 mRNA. Molecular and Cellular Neuroscience. 26, 182–190
14. Monteiro, P. and Feng, G. (2017). SHANK proteins: roles at the synapse and in autism spectrum disorder. Nature Reviews Neuroscience. 18, 147-157
15. Durand, C.M., Betancur, C., Böckers, T.M., Bockmann, J., Chaste, P., Fauchereau, F., et al (2007). Mutations in the gene encoding the synaptic scaffolding protein SHANK3 are associated with autism spectrum disorders. Nature Genetics. 39, 25–27

16. Wang, X., Xu, Q., Bey, A.L., Lee, Y. and Jiang, Y.H. (2014). Transcriptional and functional complexity of Shank3 provides a molecular framework to understand the phenotypic heterogeneity of SHANK3 causing autism and Shank3 mutant mice. Molecular Autism. 5, 30
17. Redecker, P., Gundelfinger, E.D. and Böckers, T.M. (2001). The cortactinbinding postsynaptic density protein proSAP1 in non-neuronal cells. Journal of Histochemistry & Cytochemistry. 49, 639 – 648
18. Saavedra, M.V., Smalla, K.H., Thomas, U., Sandoval, S., Olavarria, K., Castillo K, et al. (2008). Scaffolding proteins in highly purified rat olfactory cilia membranes. NeuroReport. 19, 1123–1126
19. Brandstätter, J.H., Dick, O. and Böckers, T.M. (2004). The postsynaptic scaffold proteins ProSAP1/Shank2 and Homer1 are associated with glutamate receptor complexes at rat retinal synapses. Journal of Comparative Neurology. 475, 551–563
20. Raab, M., Böckers, T.M. and Neuhuber, W.L. (2010). Proline-rich synapse-associated protein-1 and 2 (ProSAP1/Shank2 and ProSAP2/Shank3)-scaffolding proteins are also present in postsynaptic specializations of the peripheral nervous system. Neuroscience. 171, 421– 433
21. McWilliams, R.R., Gidey, E., Fouassier, L., Weed, S.A. and Doctor, R.B. (2004). Characterization of an ankyrin repeat-containing Shank2 isoform (Shank2E) in liver epithelial cells. Biochemical Journal. 380, 181–191
22. Dobrinskikh, E., Giral, H., Caldas, Y.A., Levi, M. and Doctor, R.B. (2010). Shank2 redistributes with NaPilla during regulated endocytosis. American Journal of Physiology: Cell Physiology. 299, C1324–C1334
23. Zitzer, H., Honck, H.H., Bachner, D., Richter, D. and Kreienkamp, H.J. (1999). Somatostatin receptor interacting protein defines a novel family of multidomain proteins present in human and rodent brain. The Journal of Biological Chemistry. 274, 32997–33001
24. Peça, J., Feliciano, C., Ting, J.T., Wang, W., Wells, M.F., Venkatraman, T.N., et al. (2011). Shank3 mutant mice display autistic-like behaviours and striatal dysfunction. Nature. 472, 437–442
25. Lee, J., Chung, C., Ha, S., Lee, D., Kim, D.Y., Kim, H. and Kim, E. (2015). Shank3-mutant mice lacking exon 9 show altered excitation/inhibition balance, enhanced rearing, and spatial memory deficit. Frontiers in Cellular Neuroscience. 9, 94
26. Wang, X., Bey, A.L., Katz, B.M., Badea, A., Kim, N., David, L.K. et al. (2016). Altered mGluR5-Homer scaffolds and corticostriatal connectivity in a Shank3 complete knockout model of autism. Nature Communications. 10, 7-11459
27. Ramus, S.J., Davis, J.B., Donahue, R.J., Discenza, C.B. and Waite, A.A. (2007). Interactions between the orbitofrontal cortex and the hippocampal memory system during the storage of long-term memory. Annals of the New York Academy of Sciences. 1121, 216–231
28. Lehn, H., Steffenach, H.A., Van Strien, N.M., Veltman, D.J., Witter, M.P. and Haberg, A. K. (2009). A specific role of the human hippocampus in recall of temporal sequences. Journal of Neurochemistry. 29, 3475–3484
29. Pehrs, C., Samson, A.C. and Gross, J.J. (2015). The quartet theory: implications for autism spectrum disorder: comment on “The quartet theory of human emotions: an integrative and neurofunctional model” by S. Koelsch et al. Physics of Life Reviews. 13, 77–79
30. Heise, C., Schroeder, J.C., Schoen, M., Halbedl, S., Reim, D. and Woelfle, S. (2016). Selective Localization of Shanks to VGLUT1-Positive Excitatory Synapses in the Mouse Hippocampus. Frontiers in Cellular Neuroscience. 10, 106
31. Sheng, M. and Kim, E. (2011). The postsynaptic organization of synapses. Cold Spring Harbor Perspectives in Biology. 3, a005678

32. Sheng, M. and Kim, M.J. (2002). Postsynaptic signaling and plasticity mechanisms. Science. 298, 776 –780
33. Kleijer, K.T., Schmeisser, M.J., Krueger, D.D., Böckers, T.M., Scheiffele, P., Bourgeron, T., et al. (2014). Neurobiology of autism gene products: towards pathogenesis and drug targets. Psychopharmacology (Berl). 231, 1037-62
34. Böckers, T.M., Winter, C., Smalla, K.H., Kreutz, M.R., Bockmann, J. Seidenbecher, C. et al. (1999b). Proline-rich synapse-associated proteins ProSAP1 and ProSAP2 interact with synaptic proteins of the SAPAP/GKAP family. Biochemical and Biophysical Research Communications. 264, 247–252
35. Garner, C.C., Nash, J. and Huganir, R.L. (2000). PDZ domains in synapse assembly and signalling. Trends in Cell Biology. 10, 274–280
36. Böckers, T.M. (2006). The postsynaptic density. Cell and Tissue Research. 326, 409–442
37. Romorini, S., Piccoli, G., Jiang, M., Grossano, P., Tonna, N. and Passafaro, M. (2004). A functional role of postsynaptic density-95-guanylate kinase-associated protein complex in regulating shank assembly and stability to Synapses. Journal of Neurochemistry. 24, 9391–9404
38. Böckers, T.M., Liedtke, T., Spilker, C., Dresbach, T., Bockmann, J., Kreutz, M.R. and Gundelfinger, E.D. (2005). C-terminal synaptic targeting elements for postsynaptic density proteins ProSAP1/Shank2 and ProSAP2/Shank3. Journal of Neurochemistry. 92, 519 –524
39. Tao-Cheng, J., Dosemeci, A., Gallant, P.E., Smith, C. and Reese, T. (2010). Activity Induced Changes in the Distribution of Shanks at Hippocampal Synapses. Neuroscience. 168, 11–17
40. Falley, K., Schütt, J., Iglauer, P., Menke, K., Maas, C., Kneussel, M., et al. (2009). Shank1 mRNA: dendritic transport by kinesin and translational control by the 5' untranslated region. Traffic. 10, 844 –857
41. Grabrucker, S., Proepper, C., Mangus, K., Eckert, M., Chhabra, R., Schmeisser, M.J. et al. (2014). The PSD protein ProSAP2/Shank3 displays synapto-nuclear shuttling which is deregulated in a schizophrenia-associated mutation. Experimental Neurology. 253, 126–137
42. Durand, C.M., Perroy, J., Loll, F., Perrais, D., Fagni, L., Bourgeron, T., et al. (2012). SHANK3 mutations identified in autism lead to modification of dendritic spine morphology via an actin-dependent mechanism. Molecular Psychiatry. 17, 71–84
43. Li, Z. and Sheng, M. (2003). Some assembly required: the development of neuronal synapses. Nature Reviews Molecular Cell Biology. 4, 833-841
44. McKinney, R.A., Capogna, M., Durr, R., Gahwiler, B.H. and Thompson, S.M. (1999). Miniature synaptic events maintain dendritic spines via AMPA receptor activation. Nature Neuroscience. 2, 44–49
45. Korkotian, E. and Segal, M. (1999). Release of calcium from stores alters the morphology of dendritic spines in cultured hippocampal neurons. Proceedings of the National Academy of Sciences. 96, 12068–12072
46. Roussignol, G., Ango, F., Romorini, S., Tu, J.C., Sala, C., Worley, P.F. et al. (2005). Shank Expression Is Sufficient to Induce Functional Dendritic Spine Synapses in Aspiny Neurons. The Journal of Neuroscience. 25, 3560–3570
47. Grabrucker, A.M., Vaida, B., Bockmann, J. and Böckers, T.M. (2009). Synaptogenesis of hippocampal neurons in primary cell culture. Cell and Tissue Research. 338, 333-41
48. Halbedl, S., Schoen, M., Feiler, M.S., Böckers, T.M. and Schmeisser, M.J. (2016). Shank3 is localized in axons and presynaptic specializations of developing hippocampal neurons and involved in the modulation of NMDA receptor levels at axon terminals. Journal of Neurochemistry. 137, 26-32

49. Grabrucker, A.M., Knight, M.J., Proepper, C., Bockmann, J., Joubert, M., Rowan, M. et al. (2011). Concerted action of zinc and ProSAP/Shank in synaptogenesis and synapse maturation. The EMBO Journal. 30, 569-81
50. Sala, C., Roussignol, G., Meldolesi, J. and Fagni, L. (2005). Key role of the postsynaptic density scaffold proteins shank and homer in the functional architecture of Ca^{2+} homeostasis at dendritic spines in hippocampal neurons. Journal of Neurochemistry. 25, 4587–4592
51. Berkel, S., Tang, W., Treviño, M., Vogt, M., Obenhaus, H.A. and Gass, P. (2012). Inherited and de novo SHANK2 variants associated with autism spectrum disorder impair neuronal morphogenesis and physiology. Human Molecular Genetics: Oxford Journals. 21, 344-57
52. Shen, D., Zhang, L., Wei, E. and Yang, Y. (2015). Autophagy in synaptic development, function, and pathology. Neuroscience Bulletin. 31, 416-26
53. Eagle, H., Piez, K.A., Fleischman, R. and Oyama, V.I. (1959). Protein turnover in mammalian cell cultures. Biochemical Journal. 234, 592–597
54. Alvarez-Castelão, B. and Schuman, E. (2015). The regulation of synaptic protein turnover. Biochemical Journal. 290, 28623-30
55. Blanpied, T.A., Kerr and J.M., Ehlers, M.D. (2008). Structural plasticity with preserved topology in the postsynaptic protein network. Proceedings of the National Academy of Sciences of the United States of America. 105, 12587–12592
56. Minerbi, A., Kahana, R., Goldfeld, L., Kaufman, M., Marom, S. and Ziv, N.E. (2009). Long-term relationships between synaptic tenacity, synaptic remodeling, and network activity. PLoS Biology. 7: e1000136.
57. Inoue, A. and Okabe, S. (2003). The dynamic organization of postsynaptic proteins: Translocating molecules regulate synaptic function. Current Opinion in Neurobiology. 13, 332–340
58. Malinow, R. and Malenka, R.C. (2002). AMPA receptor trafficking and synaptic plasticity. Annual Review of Neuroscience. 25, 103–26
59. Malenka, R.C. and Bear, M.F. (2004). LTP and LTD: an embarrassment of riches. Neuron. 44, 5–21
60. Schuman, E.M., Dynes, J.L. and Steward, O. (2006). Synaptic regulation of translation of dendritic mRNAs. Journal of Neuroscience. 26, 7143–46
61. Ehlers, M.D. (2003). Activity level controls postsynaptic composition and signaling via the ubiquitin-proteasome system. Nature Neuroscience. 6, 231–42
62. Brown, E.J. and Schreiber, S.L. (1996). A signalling pathway to translational control. Cell. 86, 517–520
63. Tang, S.J., Reis, G., Kang, H., Gingras, A.C., Sonenberg, N. and Schuman, E.M. (2002). A rapamycin-sensitive signaling pathway contributes to long-term synaptic plasticity in the hippocampus. Proceedings of the National Academy of Sciences of the United States of America. 99, 467–472
64. Chang, Y.Y., Juhász, G., Goraksha-Hicks, P., Arsham, A.M., Mallin, D.R., Muller, L.K. et al, (2009). Nutrient-dependent regulation of autophagy through the target of rapamycin pathway. Biochemical Society Transactions. 37, 232-6
65. Kim, J., Kundu, M., Viollet, B. and Guan, K.L. (2011). AMPK and mTOR regulate autophagy through direct phosphorylation of Ulk1. Nature Cell Biology. 13, 132-41
66. Speese, S.D., Trotta, N., Rodesch, C.K., Aravamudan, B. and Broadie, K. (2003). The ubiquitin proteasome system acutely regulates presynaptic protein turnover and synaptic efficacy. Current Biology. 13, 899–910

67. Korhonen, L. and Lindholm, D. (2004). The ubiquitin proteasome system in synaptic and axonal degeneration: a new twist to an old cycle. The Journal of Cell Biology. 165, 27–30
68. Petralia, R.S, Schwartz, C.M., Wang, Y.X., Kawamoto, E.M., Mattson, M.P. and Yao, P.J. (2013). Sonic hedgehog promotes autophagy in hippocampal neurons. Biology Open. 2, 499–504
69. Komatsu, M., Waguri, S., Ueno, T., Iwata, J., Murata, S., Tanida, I. et al. (2005).Impairment of starvation-induced and constitutive autophagy in Atg7-deficient mice. Journal Cell Biology. 169, 425-434
70. Tang, G., Gudsnuk, K., Kuo, S.H., Cotrina, M.L., Rosoklija, G., Sosunov, A. et al. (2014). Loss of mTOR-dependent macroautophagy causes autistic-like synaptic pruning deficits. Neuron. 83, 1131-43
71. Hutsler, J.J. and Zhang, H. (2010). Increased dendritic spine densities on cortical projection neurons in autism spectrum disorders. Brain Research. 1309, 83–94
72. Abrahams, B.S. and Geschwind, D.H. (2008). Advances in autism genetics: on the threshold of a new neurobiology. Nature. 9, 341-356
73. Peça, J. and Feng, F. (2012). Cellular and synaptic network defects in autism. Current Opinion in Neurobiology. 22, 866–872
74. Schaaf, C.P. and Zoghbi, H.Y. (2011). Solving the autism puzzle a few pieces at a time. Neuron. 70, 806–8
75. Freitag, C.M. (2007). The genetics of autistic disorders and its clinical relevance: a review of the literature. Molecular Psychiatry. 12, 2–22
76. Geschwind, D.H. (2009). Advances in autism. Annual Review of Medicine. 60, 367–380
77. Buxbaum, J.D. (2009). Multiple rare variants in the etiology of autism spectrum disorders. Dialogues in Clinical Neuroscience. 11, 35–43
78. Betancur, C., Sakurai, T. and Buxbaum, J.D. (2009). The emerging role of synaptic cell-adhesion pathways in the pathogenesis of autism spectrum disorders. Trends in Neurosciences. 32, 402–12
79. Devlin, B and Scherer, S.W. (2012). Genetic architecture in autism spectrum disorder. Current Opinion in Genetics & Development. 22, 229–37
80. Bonaglia, M.C., Giorda, R., Borgatti, R., Felisari, G., Gagliardi, C., Selicorni, A. et al. (2001). Disruption of the ProSAP2 gene in a t(12;22)(q24.1;q13.3) is associated with the 22q13.3 deletion syndrome. The American Journal of Human Genetics. 69, 261-8
81. Phelan, K. and McDermid, H.E. (2012). The 22q13.3 Deletion Syndrome (PhelanMcDermid Syndrome). Molecular Syndromology. 2, 186–201
82. Phelan, M.C. and McDermid, H.E. (2001). The 22q13.3 Deletion Syndrome (Phelan-McDermid Syndrome). Molecular Syndromology. 101, 91–99
83. Sato, D., Lionel, A.C., Leblond, C.S., Prasad, A., Pinto, D., Walker, S. et al. (2012). SHANK1 Deletions in Males with Autism Spectrum Disorder. The American Journal of Human Genetics. 90, 879–887
84. Berkel, S., Marshall, C.R., Weiss, B., Howe, J., Roeth, R., Moog, U., et al. (2010). Mutations in the SHANK2 synaptic scaffolding gene in autism spectrum disorder and mental retardation. Nature Genetics. 42, 489–491
85. Pinto, D., Pagnamenta, A.T., Klei, L., Anney, R., Merico, D., Regan, R. et al. (2010). Functional impact of global rare copy number variation in autism spectrum disorders. Nature. 466, 368–372
86. Leblond, C.S., Nava, C., Polge, A., Gauthier, J., Huguet, G., Lumbroso, S, et al. (2014). Meta-analysis of SHANK Mutations in Autism Spectrum Disorders: a gradient of severity in cognitive impairments. PLoS Genetics. 10, e1004580

87. Won, H., Lee, H-R., Gee, H.Y., Mah, W., Kim, J.I., Lee, J. et al (2012). Autistic-like social behaviour in Shank2-mutant mice improved by restoring NMDA receptor function. Nature. 486, 261–265
88. Schmeisser, M.J., Ey, E., Wegener, S., Bockmann, J., Stempel, A.V., Kuebler, A., et al. (2012). Autistic-like behaviours and hyperactivity in mice lacking ProSAP1/Shank2. Nature. 486, 256–260
89. Hung, A.Y., Futai, K., Sala, C., Valtschanoff, J.G., Ryu, J., Woodworth, M.A., et al. (2008). Smaller dendritic spines, weaker synaptic transmission, but enhanced spatial learning in mice lacking Shank1. The Journal of Neuroscience. 28, 1697–1708
90. Silverman, J.L., Turner, S.M., Barkan, C.L., Tolu, S.S., Saxena, R., Hung, A.Y. et al. (2011). Sociability and motor functions in Shank1 mutant mice. Brain Research. 1380, 120–137
91. Wöhr, M., Roullet, F.I., Hung, A.Y., Sheng, M. and Crawley, J.N. (2011). Communication impairments in mice lacking Shank1: reduced levels of ultrasonic vocalizations and scent marking behavior. PLoS One. 6, e20631
92. Shmelkov, S.V., Hormigo, A., Jing, D., Proenca, C.C., Bath, K.G. and Milde, T. (2010). Slitrk5 deficiency impairs corticostriatal circuitry and leads to obsessive-compulsive-like behaviors in mice. Nature Medicine. 16, 598–602
93. Welch, J.M., Lu, J., Rodriguiz, R.M., Trotta, N.C., Peça, J., Ding, J.D. (2007). Cortico-striatal synaptic defects and OCD-like behaviours in Sapap3-mutant mice. Nature. 448, 89-900
94. Mei, Y., Monteiro, P., Zhou, Y. Kim, J., Gao, X., Fu, Z. and Feng, G. (2016). Adult restoration of Shank3 expression rescues selective autistic-like phenotypes. Nature. 530, 481–484
95. Zhou, Y., Kaiser, T., Monteiro, P., Zhang, X., Van der Goes, M.S., Wang, D. et al. (2016). Mice with Shank3 mutations associated with ASD and schizophrenia display both shared and distinct defects. Neuron. 89, 147–162
96. Peixoto, R., Wang, W., Croney, D., Kozorovitskiy, Y. and Sabatini, B. (2016). Early hyperactivity and precocious maturation of corticostriatal circuits in Shank3B−/−mice. Nature Neuroscience. 19, 716–724
97. Mao, W., Watanabe, T., Cho, S., Frost, J.L., Truong, T., Zhao, X. et al. (2015). Shank1 regulates excitatory synaptic transmission in mouse hippocampal parvalbumin-expressing inhibitory interneurons. European Journal of Neuroscience. 41, 1025–1035
98. Wang, X., McCoy, P.A., Rodriguiz, R.M., Pan, Y., Je, H.S., Roberts, A.C. et al. (2011). Synaptic dysfunction and abnormal behaviors in mice lacking major isoforms of Shank3. Human Molecular Genetics 20, 3093–3108
99. Bozdagi, O., Sakurai, T., Papapetrou, D., Wang, X., Dickstein, D.L., Takahashi, N. et al. (2010). Haploinsufficiency of the autism associated Shank3 gene leads to deficits in synaptic function, social interaction, and social communication. Molecular Autism. 1, 15
100. Jaramillo, T.C., Speed, H.E., Xuan, Z., Reimers, J.M., Liu, S. and Powell, C.M. (2016). Altered striatal synaptic function and abnormal behaviour in Shank3 Exon4-9 deletion mouse model of autism. Autism Research. 9, 350–375
101. Vicidomini, C., Ponzoni, L., Lim, D., Schmeisser, M., Reim, D., Morello, N. (2016). Molecular Psychiatry. 22, 689-702
102. Kouser, M., Speed, H.E., Dewey, C.M., Reimers, J.M., Widman, A.J., Gupta, N. et al, (2013). Loss of predominant Shank3 isoforms results in hippocampus-dependent impairments in behavior and synaptic transmission. Journal of Neuroscience. 33, 18448–18468
103. Okerlund, N.D., Schneider, K., Leal-Ortiz, S., Montenegro-Venegas, C., Kim, S.A., Garner, L.C. et al. (2017). Bassoon Controls Presynaptic Autophagy through Atg5. Neuron. 93, 897-913

104. Vanhecke, D., Graber, W. and Studer, D. (2008). Close-to-native ultrastructural preservation by high pressure freezing. Methods Cell Biology. 88, 151-64
105. Filimonenko, M., Isakson, P., Finley, K.D., Anderson, M., Melia, T.J., Jeong, H. et al. (2011). The selective macroautophagic degradation of aggregated proteins requires the phosphatidylinositol 3-phosphate binding protein Alfy. Molecular Cell. 38, 265–279
106. Jung, C.H., Ro, S., Cao, J., Otto, N.M. and Kim, D. (2010). mTOR regulation of autophagy. FEBS Letters. 584, 1287–1295
107. Klionsky, A., Abdelmohsen, K., Abe, A., Abedin, M.J., Abeliovich, H., Abeliovich, H. et al. (2016). Guidelines for the use an interpretation of assays for monitoring autophagy (3rd edition). Autophagy. 12, 1-222
108. Mizushima, N. and Yoshimori, T. (2007). How to interpret LC3 immunobloting. Autophagy. 3, 542-5
109. Tanida, I., Ueno, T. and Kominami, E. (2008). LC3 and Autophagy. Methods in Molecular Biology. 445:77-88
110. Waites, C.L., Leal-Ortiz, S.A., Okerlund, N., Dalke, H., Fejtova, A., Altrock, W.D., et al. (2013). The EMBO Journal. 32, 954-969
111. Lau, C.G. and Zukin, R.S. (2007). NMDA receptor trafficking in synaptic plasticity and neuropsychiatric disorders. Nature Reviews Neuroscience. 8, 413-426
112. Prior, P., Schmitt, B., Grenningloh, G., Pribilla, I., Multhaup, G., Beyreuther, K. et al. (1992). Primary structure and alternative splice variants of gephyrin, a putative glycine receptor-tubulin linker protein. Neuron. 8, 1161-70
113. Luscher, B. and Keller, C.A. (2004). Regulation of GABA(A) receptor trafficking, channel activity, and functional plasticity of inhibitory synapses. Pharmacology & Therapeutics. 102, 195–221
114. Nagy, A. (2000). Cre recombinase: the universal reagent for genome tailoring. Genesis. 26, 99-109
115. Berkel S., Tang, W.,Trevin, M., Vogt, M., Obenhaus, H.A., Gass, P. et al. (2011). Inherited and de novoSHANK2 variants associated with autism spectrum disorder impair neuronal morphogenesis and physiology. Human Molecular Genetics. 21, 344–357
116. Kreitzer, A.C. (2005). Neurotransmission: Emerging Roles of Endocannabinoids. Current Biology. 15, 549-551